JOC The Journal of Organic Chemistry
Cite This: J. Org. Chem. 2018, 83, 1828−1841
Article
pubs.acs.org/joc

Synthesis and Characterization of Electron-Deficient Asymmetrically Substituted Diarylindenotetracenes

Lafe J. Purvis, Xingxian Gu,† Soumen Ghosh, Zhuoran Zhang, Christopher J. Cramer,* and Christopher J. Douglas*

Department of Chemistry, Chemical Theory Center, and Supercomputing Institute, University of Minnesota, Minneapolis, Minnesota 55455, United States

Supporting Information

ABSTRACT: Electron-deficient asymmetrically substituted diarylindenotetracenes were prepared via a series of Friedel−Crafts acylations, aryl−aryl cross-couplings, and an intramolecular oxidative cyclization to form the indene ring. Single-crystal X-ray experiments showed good $\pi-\pi$ overlap with $\pi-\pi$ distances ranging from 3.26 to 3.76 Å. Both thermogravimetric analysis and differential scanning calorimetry indicated that asymmetrically substituted indenotetracenes (ASIs) are stable at elevated temperatures. From cyclic voltammetry experiments, HOMO/LUMO energy levels of ASI derivatives were determined to be near −5.4/−4.0 eV. UV/visible absorption spectra showed strong absorption of light between 400 and 650 nm with molar attenuation coefficients from 10^4 to 10^5 M^{-1} cm^{-1}. ASIs were also found to have very low fluorescence quantum yields, less than 4%. Using the solid-state packing determined from the single-crystal X-ray experiments, computational modeling indicated that ASI molecules should favor electron transport.

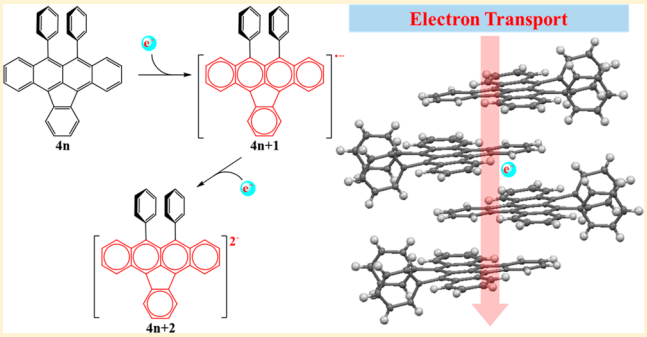

INTRODUCTION

Over the past decades, the demand for cheaper, faster, and smaller electronic devices has driven chemists to discover a large number of new small-molecule, electron-donor, p-type materials. Over the same period, however, there has been significantly less development of novel small-molecule, electron-acceptor, n-type materials, especially for use in organic solar cells.[1] To date, the benchmark electron-acceptor material for organic photovoltaics has been the fullerene C_{60}, owing to its high electron affinity and efficient isotropic charge transport.

However, despite having good solid-state properties that allow for efficient electron transport, fullerenes are not ideal materials for organic photovoltaic materials (OPVs). The several drawbacks of fullerenes include poor solubility in organic solvents, limited stability, and relatively high cost. Another drawback of fullerenes is their poor absorption of light in the visible region. In OPVs, this relative transparency necessitates a thick absorber layer in order to produce sufficient light-generated charge carriers (excitons). Although the thicker absorber layer does result in greater exciton generation, it also decreases charge separation efficiency of the device due to the short diffusion length of excitons in the organic material.[2−5]

Recently, efforts to overcome the inherent deficiencies of fullerenes led to the development of several novel non-fullerene electron acceptors.[6−13] Non-fullerene electron acceptors have the potential to greatly improve OPV performance through design of materials with strong light absorption, tuned highest occupied molecular orbital (HOMO)/lowest unoccupied molecular orbital (LUMO) levels, and improved processability and photostability.[14−16] Among these novel electron acceptors, indene-fused aromatic compounds have shown promise as possible replacements for fullerenes in OPVs.[17−19]

The intrinsic electron deficiency of indene-containing molecules originates from the electron-accepting ability of the conjugated five-membered ring. The drive toward aromaticity $(4n + 2)$ makes materials containing indenes good electron acceptors. The Plunkett group and Haley group have independently developed new organic n-type materials based on the indene scaffold for use in OPVs.[8,20,21] Corannulenes may also replace fullerenes as the electron-transport layer.[22] The cyclopentane-fused polycyclic aromatic hydrocarbons and indacene materials demonstrate LUMOs below −3.5 eV and HOMOs below −5.5 eV, allowing for n-type behavior. These materials also have good solubility in organic solvents and can be readily derivatized.

Extending the range of indene-based materials as new n-type acceptors, we have prepared and studied diarylindenotetracenes. Previously, our group reported the development of symmetrically substituted indenotetracenes.[23] In this article, we report a divergent synthetic strategy allowing for rapid diversification and structure−function relationship studies of the indenotetracene core. Our new synthetic strategy enabled us to prepare several asymmetrically substituted indenotetra-

Received: October 31, 2017
Published: January 23, 2018

DOI: 10.1021/acs.joc.7b02756
J. Org. Chem. 2018, 83, 1828−1841

Scheme 1. Synthesis of Asymmetric Indenotetracenes 8a−m

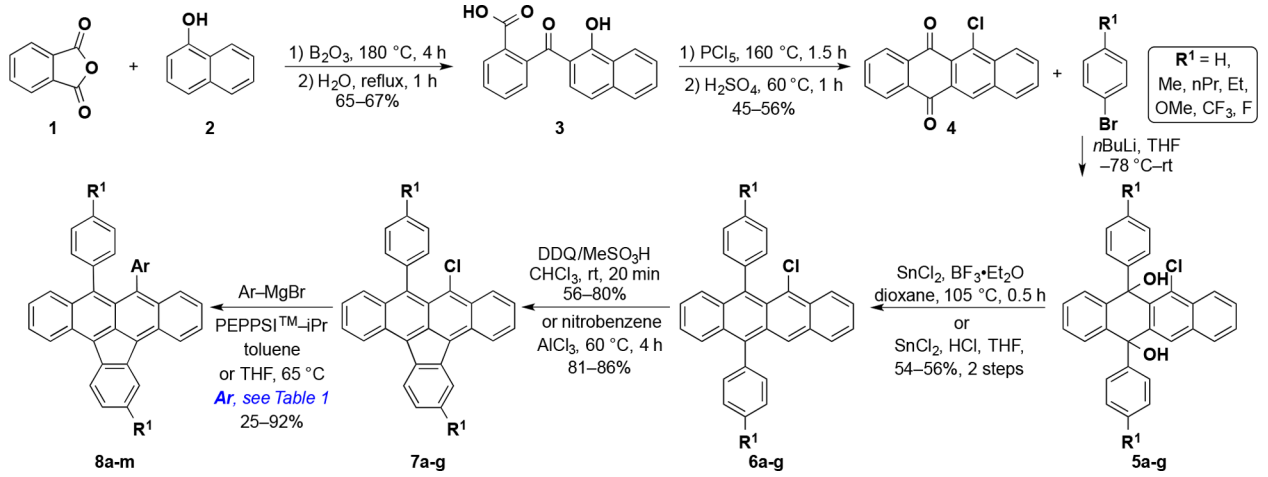

cene (ASI) derivatives. Beyond the syntheses, we have examined and modeled their electronic and physical properties to evaluate their potential for use as n-type materials in organic photovoltaics.[24]

RESULTS AND DISCUSSION

Synthesis. We began by designing the synthesis of ASIs to allow for late-stage diversification and easy derivatization. This was accomplished via a series of Friedel−Crafts acylations, aryl−aryl cross-coupling reactions, and a Scholl oxidative cyclization (Scheme 1).

Starting with commercially available phthalic anhydride (**1**) and 1-hydroxyl naphthalene (**2**), 2-(1-hydroxy-2-naphthoyl)-benzoic acid, compound **3**, was obtained via a Friedel−Crafts acylation using the Lewis acid boron trioxide. Following treatment of compound **3** with PCl_5 and heating in sulfuric acid 6-chlorotetracene-5,12-dione, compound **4** was obtained in good yields, 50% over two steps.[9] Using the above conditions, compound **4** was synthesized on 0.1 mole scale, which was then used in all subsequent syntheses. The first point of diversification was achieved by treating naphthacenequinone **4** with substituted aryllithium reagents, producing the diol intermediates **5a−g** as mixtures of *syn*/*anti* isomers. Upon reductive aromatization, compounds **6a−g** became a bright orange/red color, indicating that the tetracene core had been successfully formed (Table 1).[25,26]

In the key step of our synthesis, we envisioned forming the indene ring via an oxidative cyclization using Scholl reaction conditions.[27,28] In previous syntheses of rubicene and other indene-containing polycyclic aromatic hydrocarbons (PAHs), the indene moieties were prepared via intramolecular palladium-catalyzed aryl−aryl cross-coupling or pentannulation.[29,30] Scholl reaction conditions have been used in the synthesis of several PAH compounds, and recently, Chi and coworkers synthesized bisindeno-annulated pentacene molecules under Scholl reaction conditions using $FeCl_3$ as the oxidizing agent.[31,32] Using two different Scholl reaction conditions, compounds **7a**,**b** were formed via oxidative cyclization using $AlCl_3$ in nitrobenzene, whereas compounds **7c−g** were obtained from a solution of chloroform and methanesulfonic acid in the presence of 2,3-dichloro-5,6-dicyano-1,4-benzoquinone (DDQ), with yields ranging from 40 to 86%.[33,34] The formation of compounds **7a−g** resulted in another color change, from the orange/red color of compounds **6a−g** to a purple/black color. Interestingly, the regiochemsitry of compounds **7a−g** was found to be very specific. Oxidative cyclization was only observed to occur at the C12 of the tetracene core and never at the C10. We attributed this high regioselectivity to steric repulsion between the C5 chloride and the C6 phenyl group. This steric repulsion pushes carbons 5 and 6 away from each other, which, in turn, pushes the C11 phenyl group closer to the C12 hydrogen.

From compounds **7a−g**, we performed the final late-stage diversification, using Kumada−Corriu cross-coupling conditions previously developed in our lab, to produce compounds **8a−m** in yields between 40% and 92%.[23,35,36] We found that, in most cases, the primary impurities in the crude reaction mixtures were the unreacted starting material and dehalogenated compound **7**. These impurities were readily separable from the desired product by either column chromatography and/or recrystallization, the only exception being compound **8d**.[37] We were unable to find purification conditions which separated unreacted starting material **7d** from product **8d**. In order to obtain pure **8d**, the reaction had to be driven to

Table 1. Functional Groups at R^1 and Ar, Yield of Three Key Steps, and Preparation of 6−8

entry	R^1	**6**, % yield	**7**, % yield	Ar	**8**, % yield
1	H	**6a**, 80[a]	**7a**, 81	Ph[c]	**8a**, 60
2	H			*p*-C_6H_4F[c]	**8h**, 51
3	H			*p*-tol[c]	**8i**, 67
4	H			1-naphthyl[c]	**8j**, 45
5	H			4-$NMe_2C_6H_4$[c]	**8k**, 47
6	H			4-$OMeC_6H_4$[c]	**8l**, 88
7	Me			Ph[c]	**8b**, 40
8	Me	**6b**, 88[a]	**7b**, 86	4-$NMe_2C_6H_4$[c]	**8m**, 67
9	Me			*p*-C_6H_4F[c]	**8n**, 25
10	F	**6c**, 53[b]	**7c**, 81	Ph[c]	**8c**, 90
11	CF_3	**6d**, 46[b]	**7d**, 40	Ph[d]	**8d**, 92
12	OMe	**6e**, 65[b]	**7e**, 69	Ph[c]	**8e**, 54
13	Et	**6f**, 73[a]	**7f**, 67	Ph[c]	**8f**, 74
14	^{n}Pr	**6g**, 80[a]	**7g**, 47	Ph[c]	**8g**, 74

[a]Reduction using $SnCl_2$ in THF, 1 M HCl at room temperature 1 h. [b]Reduction using $SnCl_2$ in dioxane, $BF_3{\cdot}Et_2O$ at 105 °C for 20 min. [c]Palladium-catalyzed cross-coupling using PEPPSI-^{i}Pr in THF at 65 °C. [d]Palladium-catalyzed cross-coupling using PEPPSI-^{i}Pr in toluene at 65 °C.

DOI: 10.1021/acs.joc.7b02756
J. Org. Chem. 2018, 83, 1828−1841

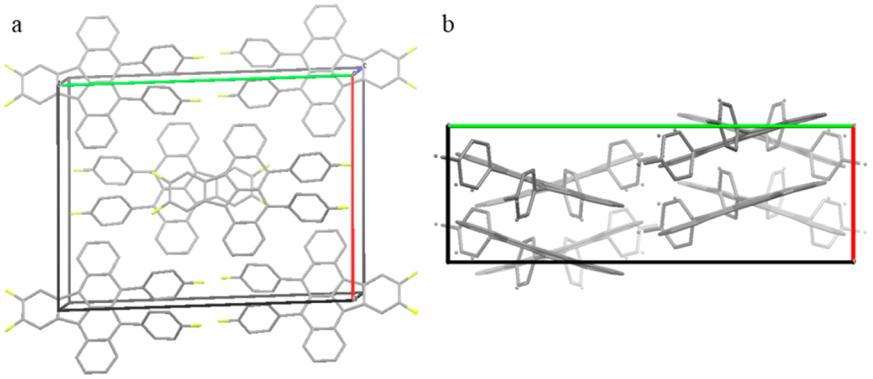

Figure 1. (a) $C2/c$ slipped 1-D π-stack in **8c** and (b) *Pbca* π-stacked herringbone in **8b**.

completion and then recrystallization could be performed to remove any additional impurities.

MATERIAL CHARACTERIZATION

Crystal Structure. In small-molecule-based OPVs, exciton dissociation and electron transport generally occurs via Dexter energy transfer.[38] For Dexter energy transfer to occur, tight packing and good orbital overlap is required between neighboring molecules in the solid state. Therefore, determining the packing in the solid state is critical to understand how a material will function as an organic semiconductor. To examine the solid-state packing of ASIs, single crystals were grown for X-ray diffraction experiments. Single crystals of ASIs were grown as small, purple, plate-like crystals via either vacuum sublimation or physical vapor transport using argon as the carrier gas.

Three packing motifs were observed with ASIs: monoclinic $C2/c$ or $P2_1/c$ and orthorhombic *Pbca*.[39] The parent symmetric compound **8a** packed in the monoclinic $C2/c$ space group.[23] Substitution of hydrogens with isosteric fluorines, as in **8c** and **8h**, also resulted in the same $C2/c$ space group. When larger functional groups were introduced, however, the crystal packing changed to monoclinic $P2_1/c$ for **8d** and **8e** and orthorhombic *Pbca* for **8b**.[40] A range of close contact distances between neighboring molecules was observed in all ASIs due to a slight twisting of the indenotetracene core ranging from 0.70° in **8e** to 9.67° in compound **8h**. Average π-stacking distances were determined by generating a plane through the ASI molecule using the atoms of the indene ring (Supporting Information (SI) section S3) and then measuring the distances between neighboring planes. The monoclinic $C2/c$ crystals showed a slipped 1-D packing (Figure 1a), with good overlap of the indenotetracene core and small $\pi-\pi$ close contacts averaging around 3.4 Å (**8a**, **8c**, and **8h**, Table 2), which would allow for efficient electron transport.[41] In the solid state, compound **8b** (orthorhombic *Pbca*) was observed to pack in a π-stacked herringbone motif (Figure 1b). Again, we observed good overlap of the indenotetracene cores with $\pi-\pi$ distances that averaged 3.46 Å and a closest contact measuring 3.36 Å. In the monoclinic $P2_1/c$ systems, compound **8e** showed little overlap of the indenotetracene core due to a horizontal displacement along the indenotetracene backbone; compound **8d**, however, demonstrated good overlap (SI section S3). Compound **8d** was also unique in that it contained two molecules in the asymmetric unit, giving two different $\pi-\pi$ close contacts, 3.28 and 3.26 Å. Compounds for which we obtained single-crystal X-ray data were further studied for their electrochemical, optical, and physical properties.

Table 2. Single-Crystal Packing Motifs for Compound 8a–e,h and Corresponding Tetracene Backbone $\pi-\pi$ Distances

crystal system	packing motif	compound	π-spacing (Å)
monoclinic	$C2/c$	**8a**	3.42
	$C2/c$	**8c**	3.42
	$C2/c$	**8h**	3.37
	$P2_1/c$	**8d**	3.26/3.28[a]
	$P2_1/c$	**8e**	3.76
orthorhombic	*Pbca*	**8b**	3.46

[a]Compound **8d** contains two molecules in the asymmetric unit with different $\pi-\pi$ distances.

Thermal Stability. To determine thermal stability and decomposition temperatures, we submitted compounds **8a–e,h** to thermogravimetric analysis studies. Shown in Table S2, compounds **8a,c,d** demonstrated no more than 1% mass loss below 300 °C, due to sublimation, whereas **8b,e,h** did not reach 1% mass loss until above 300 °C. All ASIs demonstrated good thermal stability measuring less than 5% mass loss below 325 °C and possessing onset temperatures greater than 343 °C.[6,42,43] With **8a–e,h** demonstrating good thermal stability, we next performed differential scanning calorimetry (DSC) to examine phase transitions.[10,15] Complete DSCs for each compound can be found in SI section S3. The DSC data for compounds **8a–d,h** showed no phase change between 0 to 150 °C (Figure 2). Compound **8e** showed a reversible thermal expansion at 115 °C (Figure 2). Upon further heating to 260 °C, compounds **8b–e,h** showed multiple endothermic events, suggesting the formation of alternative polymorphs at elevated temperatures. The measured thermal stability of ASIs is adequate to resist decomposition or phase changes at typical OPV device operating temperatures.

Electrochemical Properties. As stated previously, indenotetracenes possess an electron-deficient π-system due to the electronic configuration imposed by the five-membered ring. Two-electron reduction has been observed in other indene-containing molecules.[1,8,44,45] The HOMO and LUMO levels of **8a–e,h** were determined via cyclic voltammetry (CV) referenced to ferrocene (4.8 eV versus vacuum) (Figure 3). HOMO/LUMO levels were estimated from the onset of the oxidation and reduction peaks (SI section S5).[42]

All ASI derivatives showed at least two reversible, or quasi-reversible, reduction and one oxidation red–ox couples. From CV experiments, the energy levels of the LUMO, to which a first electron is added, were determined to be around −4.1 eV,

DOI: 10.1021/acs.joc.7b02756
J. Org. Chem. 2018, 83, 1828–1841

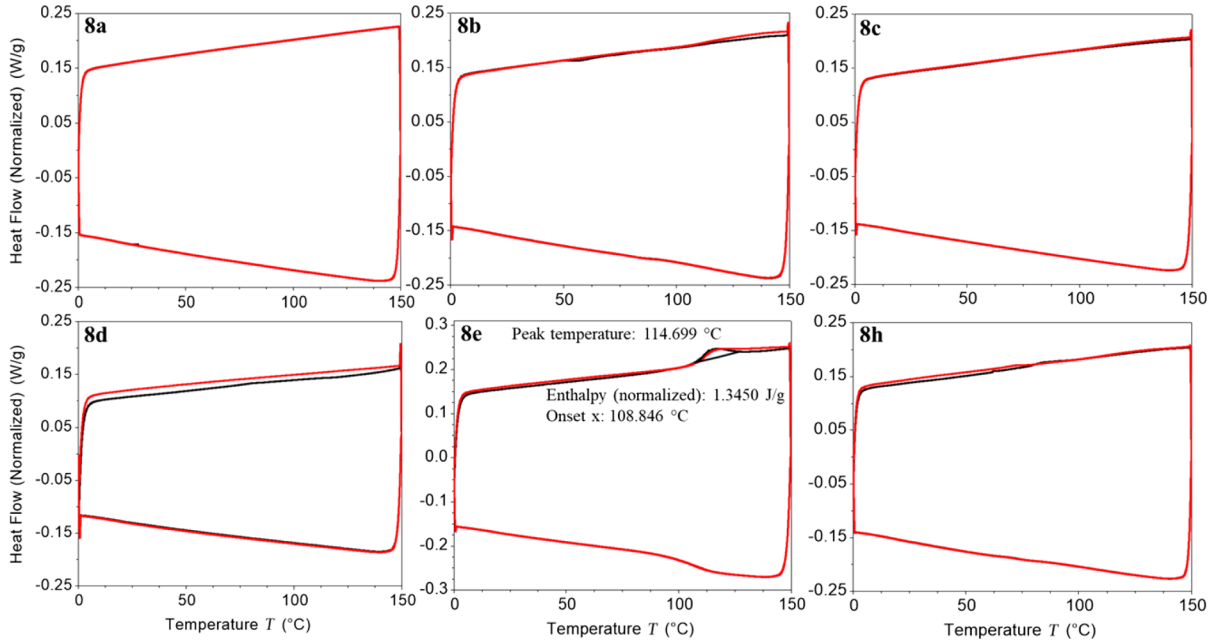

Figure 2. Differential scanning calorimetry results for compounds **8a–e,h**.

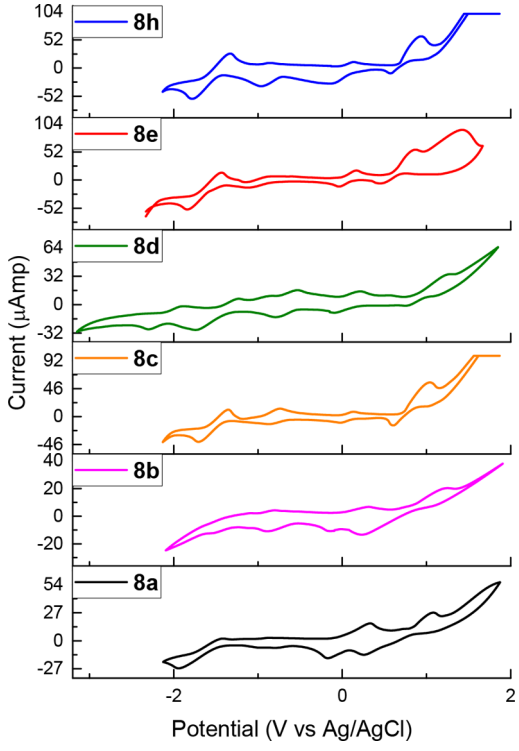

Figure 3. Cyclic voltammogram of compounds **8a–e,h**, Fc/Fc^+ used as standard. Compounds **8a,b,d,e** were run at a scan rate of 0.2 V/s and compounds **8c,h** at 0.1 V/s.

while addition of the second electron occurred between −3.27 and −3.42 eV (Table 3). The low reduction potentials of ASIs, $E_{1/2}$ = −0.9 to −0.6 V, demonstrate the high electron affinities of these molecules. All ASIs showed at least one oxidation peak near $E_{1/2}$ = 0.7 V. Estimated HOMO energy levels measured for ASIs range from −5.40 to −5.67 eV. The HOMO/LUMO energies determined for ASIs were comparable to those determined in other indene-based electron acceptors.[8,45,46]

We adjusted the HOMO/LUMO energies of ASIs via substitution around the indenotetracene core. The addition of an electron-donating methoxy group, compound **8e**, raised both the HOMO and LUMO in energy. The increased electron density of the indenotetracene core raised the HOMO energies to such a degree that a second oxidation peak could now be observed (Figure 3). Upon addition of CF_3 groups, **8d**, the measured HOMO energy decreased to −5.67 eV while addition of the first and second electron into the LUMO decreased to −4.25 and −3.42 eV, respectively. Compound **8d** also now shows a third reduction which occurred at −2.67 eV. The band gaps calculated from the measured HOMO/LUMO energy levels are shown in Table 3. The energy gaps determined from CV were found to be in good agreement with the calculated energies (SI Table S16).

The modulation of HOMO/LUMO levels of ASI via substitution with electron-donating and electron-withdrawing groups can be understood by examining the corresponding orbital amplitudes (Figure 4) determined from density functional theory (DFT) calculation. Figure 4 shows that rather than being localized to one section of the molecule (e.g., the tetracene unit), both the HOMO and LUMO are delocalized throughout the entire indenotetracene π-system. The HOMO/LUMO energies determined for the ASIs are within the range that would favor electron-accepting or ambipolar character for charge transport.[47] The higher LUMO energy levels for electron injection into indenotetracenes, compared to that measured for C_{60}, −4.5 eV, would potentially increase the open circuit voltage of an OPV by increasing the difference between the HOMO of the donor and the LUMO of the acceptor.[48−50]

Optical Properties. A major disadvantage of fullerenes is their poor absorptivity of visible light.[14] Having both the donor and acceptor layers being strong absorbers would lead to the creation of more light-generated carriers, increasing short circuit current, improving organic solar cell performance.[48,49,52]

UV/visible absorption spectroscopy of compounds **8a–e,h** showed strong absorbance over a large range of the visible

DOI: 10.1021/acs.joc.7b02756
J. Org. Chem. 2018, 83, 1828−1841

Table 3. Onset Potentials, Measured HOMO/LUMO Energies for Compounds 8a−e,h, Compared to Fc/Fc^+, and Energy Gap

compound	$E_{ox/onset}$ (1 V)	$E_{red/onset}$ (1 V)	$E_{red/onset}$ (2 V)	HOMO (eV)	LUMO (eV)	E_g (eV)	LUMO second electron (eV)	E_g (eV)
8a	0.72	−0.62	−1.47	−5.52	−4.18	1.34	−3.35	2.17
8b	0.74	−0.60	−1.50	−5.54	−4.20	1.34	−3.30	2.24
8c	0.72	−0.65	−1.42	−5.52	−4.15	1.37	−3.38	2.14
8d	0.87	−0.55	−1.38	−5.67	−4.25	1.42	−3.42	2.25
8e	0.60	−0.81	−1.53	−5.40	−3.99	1.41	−3.27	2.13
8h	0.68	−0.65	−1.48	−5.48	−4.15	1.33	−3.32	2.16

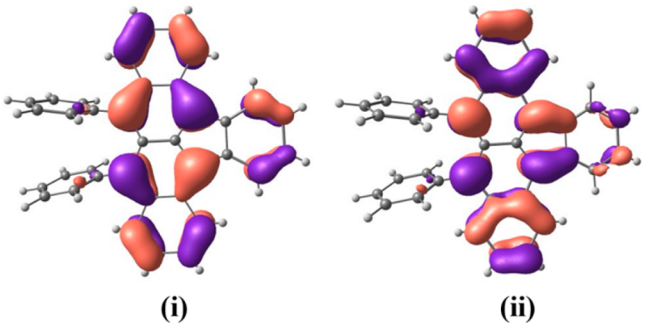

Figure 4. Orbital pictures for (i) HOMO and (ii) LUMO for **8a** (single point with M06-2X/6-31+G(d,p)).[51]

spectrum, 390−650 nm (SI section S7). All compounds showed very similar absorbance spectra with minor differences in peak shape (Figure 5). The variations in peak shape are

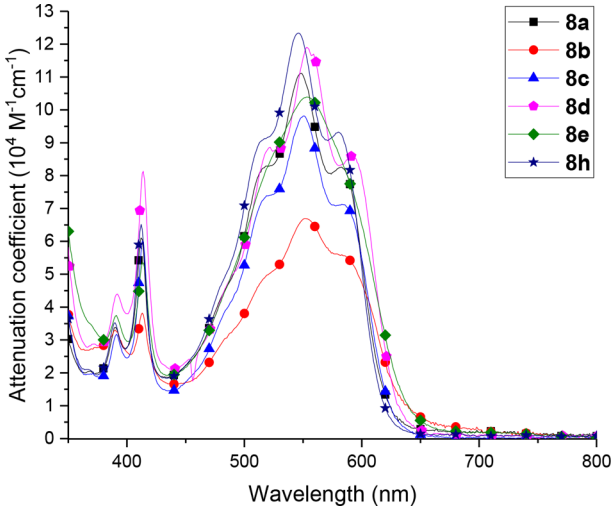

Figure 5. Absorption spectra of compounds **8a−e,h** (10^{-5} M).

attributed to the difference in bond vibrational modes/energies and intermolecular interaction between the ASI derivatives. ASIs demonstrated a strong high-energy absorption around 299 nm and weaker midrange absorption, 350−500 nm, which correspond to $\pi-\pi^*$ transitions of the ASI molecules.[43,53,54] Absorption from 450 to 650 nm is similar to that of other reported indene compounds, resulting from the charge-transfer band, indicating some $\pi-\pi$ interaction between molecules in solution.[16,20,46] The molar attenuation coefficient determined for compounds **8a−e,h** (SI Tables S9−S14) is comparable to that of ruthenium dipyridyl complexes and other materials used in dye-sensitized solar cells, which have molar attenuation coefficients around 10^4 M^{-1} cm^{-1} in the visible region.[55] The energy gaps calculated from the charge-transfer band, λ_{onset} (Table 4), for **8a−e,h** were around 1.9 eV. This agrees with those calculated from CV measurements (Table 3) and

Table 4. Values of λ_{max} and Optical Band Gaps

compound	λ_{max} (nm)	E_g (eV)[a]
8a	550	1.98
8b	553	1.86
8c	551	1.93
8e	553	1.96
8d	555	1.89
8h	546	1.98

[a]Optical band gap was calculated using the equation, $E_g = hc/\lambda$, where h is Planck's constant, c is the speed of light constant, and λ is the absorption onset.

theoretical linear-response time-dependent density functional theory (LR-TDDFT) calculations (Table S16).

Comparing the absorbance of ASI molecules to symmetrically substituted indeotetracenes, we observed that both have similar molar attenuation coefficients, between 10^4 and 10^5 M^{-1} cm^{-1}. This is to be expected due to the fact that π-conjugation of the indenotetracene core is the same.[23]

Fluorescence is the most common path for exciton decay in organic materials and can decrease OPV efficiency by decreasing exciton (Dexter) energy transfer. Figure 6 shows the absorbance and corresponding fluorescence spectra of compounds **8a−e,h**. Derivatives **8a−e,h** demonstrated weak fluorescence from 600 to 800 nm, which is common for similar indene-containing molecules.[8] The fluorescence quantum yields for compounds **8a−e,h** (Table 5) were all less than 4%.

A portion of the very low Φ can be attributed to reabsorbance due to partial overlap of the absorption and fluorescence spectra. The lack of any significant fluorescence indicates that nonradiative decay pathways, which may include intersystem crossing and/or intermolecular charge transfer, are occurring.[6,54,56] If operative, these alternate decay pathways could increase the efficiency of OPVs in which ASIs are used as the electron-accepting layer due to the possible generation of longer lived excitons as well as faster exciton dissociation.[10,15,57]

Theoretical Modeling of Electronic Structure of ASI and Charge Transport in the Solid State. To understand excited-state properties of ASIs, LR-TDDFT calculations were performed. As stated previously, the LR-TDDFT calculations for singlet and triplet energies agreed well with those determined experimentally. Singlet−triplet energy gaps in ASIs also suggest the possibility of singlet fission occurring in these molecules. Singlet fission is a process where one singlet exciton is converted into two triplet excitons in a spin-allowed process. For singlet fission to occur, transition from the singlet excited state to the multiexcitonic state with two correlated triplet excitons must be exoergic or at least isoergic, $E_S \geq 2E_T$. For compound **8a**, $E_S - 2E_T$ is 0.1 eV (0.96 kJ/mol). The same

DOI: 10.1021/acs.joc.7b02756
J. Org. Chem. 2018, 83, 1828−1841

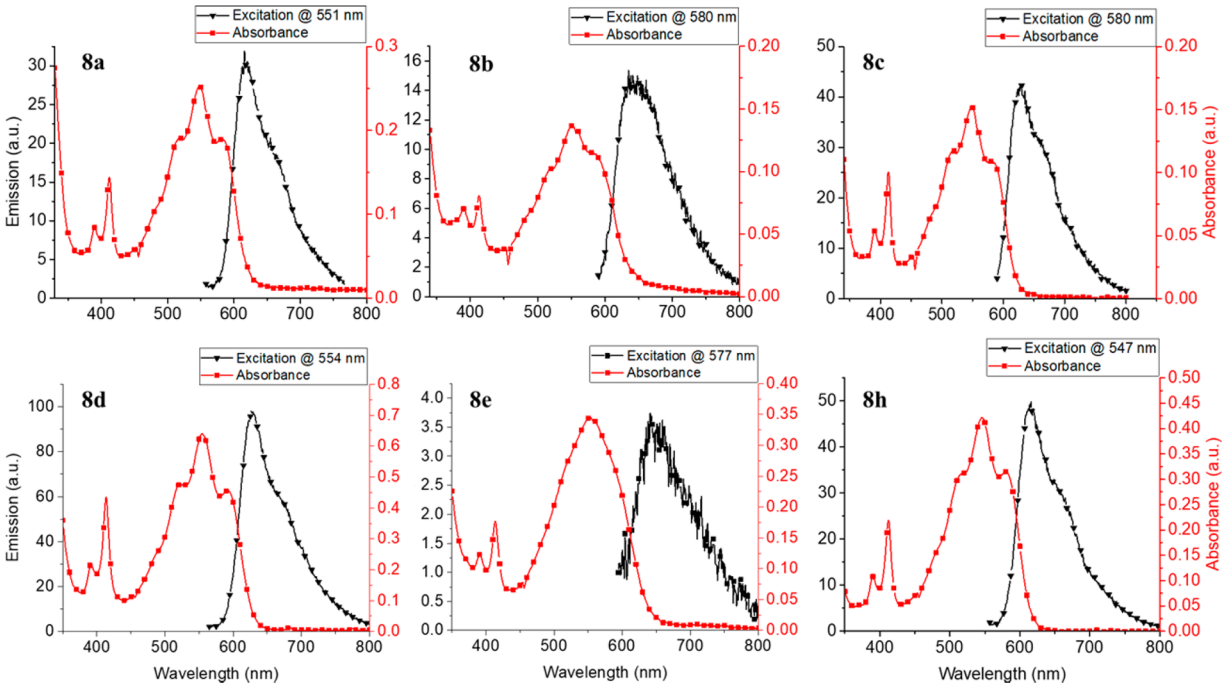

Figure 6. Fluorescence and corresponding absorbance spectra compounds **8a−e,h**.

Table 5. Calculated Fluorescence Quantum Yield for Compounds 8a−e,h Relative to Rhodamine B

compound	Φ
rhodamine B	0.7
8a	0.018
8b	0.016
8c	0.042
8d	0.029
8e	0.0015
8h	0.018

Table 6. Absolute Values for Effective Transfer Integral (meV, PBE0/6-31G(d)) Predicted for Compounds 8a−e,h[65]

compounds	crystal packing	transfer integrals, electron (meV)	transfer integrals, hole (meV)
8a	*C*2/*c*	32	5
8b	*Pbca*	34	4
8c	*C*2/*c*	19	28
8d	$P2_1/c$	87/53[a]	82/81[a]
8e	$P2_1/c$	19	57
8h	*C*2/*c*	44	7

[a]Compound **8d** contains two molecules in the asymmetric unit with slightly different $\pi-\pi$ distances. Transfer integrals were calculated for both distances.

relationship was also found for compounds **8b−e,h** (Table S16).[58] Singlet fission has been observed in other acenes and is thought to be highly beneficial for increasing the efficiency of OPVs.[59−61]

The hole and electron reorganization energies were computed for ASI derivatives **8a−e,h** and found to be comparable (see SI).[62] For each compound, **8a−d,h**, the hole reorganization energy was found to be slightly smaller than the electron reorganization energy, except for **8e**. The presence of the methoxy group in **8e** significantly increased the hole reorganization energy compared to that of **8a−d,h**, while leaving the electron reorganization energy unchanged.

Hole- and electron-transfer integrals were computed for compounds **8a−e,h** using dimer models developed from the solved single-crystal X-ray structures of each compound (Table 6; see SI section S2 for dimer pictures). For compounds **8a** and **h**, *C*2/*c* crystal structures with 1-D brick packing, the electron-transfer integral was determined to be significantly higher than the hole-transfer integral. However, in the case of compound **8c**, also *C*2/*c* and 1-D brick packing, the hole- and electron-transfer integrals were comparable. Compound **8b**, with *Pbca* packing, had an absolute electron-transfer integral significantly higher than the hole-transfer integral. The $P2_1/c$ crystal system gave two very different results depending on the substitution. Methoxy-substituted ASI **8e** had a hole-transfer integral 3 times larger than the electron-transfer integral; however, CF_3-substituted ASI **8d** had comparable hole- and electron-transfer integrals.

Calculated electron-transfer integrals for perylene diimides, a proven small-molecule electron-transport material, range from 10 to 200 meV, depending on the functional group and the model used.[63,64] The computed transfer integrals for **8a−d,h** were found to be comparable to those observed for perylene diimides. When considering both the reorganization energies and charge transfer integrals, theoretical calculations predict that compounds **8a−d,h** could function as either an electron-transport or ambipolar material, allowing them to function as n-type semiconductors in OPVs.

CONCLUSION

In summary, a new class of electron-transport material based on the indene scaffold, asymmetrically substituted indenotetracenes, has been successfully prepared. Electrochemical and thermal characterizations demonstrate the potential of ASIs as a novel electron-transport material in OPVs. ASIs were shown to strongly absorb over a broad range of the visible spectrum, with little to no concomitant fluorescence, potentially increasing

DOI: 10.1021/acs.joc.7b02756
J. Org. Chem. 2018, 83, 1828−1841

short circuit current. The higher LUMO levels of ASIs relative to C_{60} should allow for increased open circuit voltage. ASIs also demonstrated good thermal stability, which could improve OPV lifetime. Single-crystal X-ray diffraction experiments showed tight π-stacking and good backbone overlap in the solid state, allowing for efficient charge transport in the solid state. Using the solved crystal structure, ASIs were predicted to have either electron-transport or ambipolar character in organic photovoltaic devices.

Our findings demonstrate the potential of asymmetrically substituted indenotetracenes to function as a novel class of non-fullerene electron-transport materials in organic photovoltaics with the potential to improve device lifetime and efficiency.

EXPERIMENTAL SECTION

Materials and Reagents. All materials were purchased through commercial sources. THF was distilled from sodium and benzophenone. Toluene was distilled from CaH_2. 2-(1-Hydroxy-2-naphthoyl)-benzoic acid (**3**) and 6-chlorotetracene-5,12-dione (**4**) were synthesized using a previously published procedure.[9]

Measurements and Characterization. Melting temperatures for all compounds were performed on samples precipitated from solution. The melting temperature is defined as the temperature at which the powder anneals to a film rather than a free-flowing liquid. High-resolution mass spectrometry (HRMS) using GC-MS was performed on a quadrupole time-of-flight mass spectrometer with a solid injection probe. Method: inlet temperature 250 °C, source temperature 280 °C. The initial temperature was 80 °C and increased to 325 °C over 6 min and then was held for 2.3 min. HRMS using ESI was performed on time-of-flight instruments.

^{1}H NMR (300, 400, or 500 MHz), ^{13}C NMR (75, 100, or 125 MHz), and ^{19}F NMR (282 or 470 MHz) spectra were recorded on FT NMR instruments. All NMR spectra were reported as δ values in parts per million referenced to chloroform (7.26 ppm), methylene chloride (5.32 ppm), or tetramethylsilane (TMS, 0.00 ppm) for ^{1}H, chloroform (77.00 ppm) for ^{13}C, and hexafluorobenzene (−163.00 ppm) for ^{19}F NMR. Some ^{13}C NMR spectra are reported to the nearest 0.01 ppm due to the large number of close signals.

Infrared (IR) spectra were obtained as films on NaCl plates using an infrared spectrophotometer in transmission mode.

X-ray diffraction experiments were performed via single-crystal XRD using a diffractometer with graphite monochromator using Cu Kα radiation (λ = 1.5418) at 123 K ω scans and Mo Kα radiation (λ = 0.71073) at 298 K ω scans. Crystals of **8a,d,c,h** were grown via physical vapor transport (PVT) using the following technique: the temperature of the sublimation region was adjusted for each compound and ranged between 150 and 230 °C, depending on the compound. The crystal growth was held between 140 and 200 °C. The thermal gradient in the crystal growth region was created by wrapping thermal tape at continually wider intervals down the crystal growth region. Argon was used as the carrier gas. Argon flow rate was set via an oil bubbler at one bubble in the oil bubbler every 1 to 2 s. The crystals were grown in the PVT chamber over a 1−3 day period. Crystals of **8b,c** were grown via sublimation between 180 and 200 °C over 3 days under high vacuum. In the solid state, compounds **8a−c,h** were configurationally disordered, resulting in having to place the substitutions symmetrically about the diarylindenotetracene core with 50% occupancy.

Differential scanning calorimetry experiments were performed by heating compounds **8a−e,h** to 150 °C at 10 °C/min for two cycles and then heating to 260 °C in a differential scanning calorimeter.

Thermogravimetric analysis was performed by heating samples from 24 to 550 °C at a rate of 10 °C/min in a nitrogen atmosphere.

Cyclic voltammetry measurements were performed at 5 mM in anhydrous tetrahydrofuran previously degassed with argon. A silver/silver chloride reference electrode, gold working electrode, and platinum ground were used for CV experiments. Tetrabutylammonium perchlorate was used as the electrolyte and ferrocene as the standard. Cyclic voltamagrams were collected at varying concentrations and sweep rates with all showing similar red/ox character. Ferrocene oxidation onset was referenced to zero.

Absorbance measurements were performed on a UV/visible spectrometer, scanned from 1000 to 100 nm as follows: indenotetracene compounds **8a−e,h** were dissolved in dichloromethane (10 mL). Serial dilutions were performed in a factor of 10 increments (10^{-3}, 10^{-4}, 10^{-5}, 10^{-6} M), and absorbance was measured. Serial dilutions were performed using a 10 mL volumetric flask and 1 mL volumetric pipet. Attenuation coefficients (ε) were calculated from absorbance spectra corrected for dichloromethane.

Fluorescence experiments were performed on a fluorescence spectrophotometer in either ethanol or dichloromethane. The fluorescence quantum yield was calculated using rhodamine B in ethanol excited at 510 nm. The quantum yield for rhodamine B under these conditions was previously reported, Φ = 0.7.[66,67] Absorption and fluorescence measurements for compounds **8a−e,h** were performed at 10^{-5} M.

Computational Methodology. *Monomer.* We optimized monomer geometries for neutral, radical cation, and anion species in the gas phase using the M06-L exchange-correlation and 6-31+G(d,p) basis set.[51] Vibrational frequency analyses were done to confirm that all structures are minima. LR-TDDFT calculations were performed on neutral optimized geometries in the gas phase using the M06-2X exchange-correlation functional and 6-31+G(d,p) basis set.

Dimer. We used dimer models to elucidate the transfer of holes and electrons through the specific packing arrangements of different diarylindenotetracene derivatives. We extracted dimer models from experimental crystal structures of different diarylindenotetracene derivatives. Subsequently, we constrained the backbone of the diarylindenotetracene derivatives and optimized peripheryl aryl groups and the substituents. It is important to perform these constrained optimizations as there are often uncertainities in the crystal structures related to the position of the peripheryl aryl group and the substituents. Constrained optimization of dimers was performed using the PBE functional and 6-31G(d,p) basis set.[68] Damped dispersion effects were included with the pairwise D3 correction of Grimme et al. and the damping function of Becke and Johnson.

Optimized dimer geometries were used to calculate charge-transfer integrals and were accomplished using the PBE0/6-31G(d) level of theory and the fragment molecular orbital (FMO) approach. In the FMO approach, a dimer Fock matrix is constructed in the basis of monomer orbitals. Off-diagonal elements of the Fock matrix are $t_{mn} = \langle \varphi_m | h_{KS} | \varphi_n \rangle$, where φ_i represents the fragment molecular orbitals and i represents the sites (m or n). For the matrix elements relevant to the hole- (or the electron-) transfer integral between the mth and nth sites in a system, φ_m and φ_n are the HOMOs (or LUMOs) of mth and nth site, respectively. Here, as we are using a dimer model, sites represent individual monomers and h_{KS} is the Kohn−Sham Fock operator. Diagonal elements of the Fock matrix are site energies, $\varepsilon_i = \langle \varphi_i | h_{KS} | \varphi_i \rangle$. S_{mn} is the overlap matrix element between orbitals φ_m and φ_n. Since the Fock matrix is constructed here by using non-orthogonal monomer orbital basis, the effective transfer integral (t_{mn}^{eff}) is calculated using the formula

$$t_{mn}^{eff} = \frac{t_{mn} - \frac{1}{2}(\varepsilon_m + \varepsilon_n)S_{mn}}{1 - S_{mn}^2} \quad (1)$$

All optimizations of monomers and dimers and LR-TDDFT calculations were performed using the Gaussian09 software.[69] Transfer integral calculations were performed using a developer version of NWChem.[70]

Synthesis. *6-Chloro-5,12-diphenyl-5,12-dihydrotetracene-5,12-diol (**5a**).* To a flame-dried 250 mL round-bottom flask were added bromobenzene (3.23 mL, 30.8 mmol) and 30 mL anhydrous tetrahydrofuran (THF) under nitrogen. The solution was cooled to −78 °C and then *tert*-butyllithium (1.7 M, 36.2 mL, 61.5 mmol) was added dropwise to the stirring solution. The slurry was stirred at −78 °C for 1 h, then warmed to 0 °C, and the resultant phenyllithium was used immediately. To a flame-dried 500 mL round-bottom flask were

DOI: 10.1021/acs.joc.7b02756
J. Org. Chem. 2018, 83, 1828−1841

added 6-chloro-5,12-naphthacenequinone **4** (1.50 g, 5.12 mmol) and 150 mL of anhydrous THF under nitrogen. The suspension was cooled to −78 °C, and the solution of phenyllithium, prepared earlier, was added slowly. The suspension turned green and became a homogeneous solution upon the completion of addition. The solution was stirred at −78 °C for 1 h, warmed to room temperature, and stirred for 14 h. The reaction was quenched with 1 N HCl (100 mL) and extracted with EtOAc (2 × 50 mL). The organic layers were combined, washed sequentially with saturated $NaHCO_3$ (50 mL) and brine (20 mL), dried over anhydrous Na_2SO_4, and concentrated under vacuum. The crude product was carried forward without further purification.

*5-Chloro-6,11-diphenyltetracene (**6a**).* The resultant residue, compound **5a**, was dissolved in 15 mL of THF. To the resulting solution, a saturated solution of $SnCl_2$ (6.80 g, 35.9 mmol) in concentrated HCl (approximately 10 mL) was added slowly, forming a red solid which precipitated upon addition. The slurry was stirred for an additional 1 h upon complete addition of $SnCl_2$. The reaction was quenched by pouring the slurry into H_2O (200 mL). The red solid was collected by vacuum filtration. The filtrate was recrystallized from a hot solution of toluene/isopropyl alcohol (1:10) to give **6a** as a red/orange solid (1.70 g, 4.10 mmol, 80%): mp 188−189 °C; ^{1}H NMR (300 MHz, $CDCl_3$) δ 8.38 (d, J = 9.1 Hz, 1H), 8.32 (s, 1H), 7.75 (d, J = 8.5 Hz, 1H), 7.71−7.58 (m, 5H), 7.57−7.50 (m, 5H), 7.50−7.39 (m, 3H), 7.36−7.29 (m, 1H), 7.28−7.22 (m, 2H); ^{13}C NMR (75 MHz, $CDCl_3$) δ 142.1, 139.3, 138.2, 136.0, 131.8, 131.5, 131.4, 130.6, 130.1, 130.0, 129.2, 128.8, 128.6, 127.8, 127.7, 127.4, 127.0, 126.8, 126.5, 125.2, 125.1, 125.0 (not all carbon signals are resolved); IR (KBr) ν 3040, 1598, 1387, 1361, 1238 cm^{-1}; HRMS (ESI-TOF) m/z [M]$^+$ calcd for $C_{30}H_{19}Cl$ 414.1175; found 414.1171.

*9-Chloro-10-phenylindeno[1,2,3-fg]tetracene (**7a**).* To a flame-dried 100 mL round-bottom flask were added anhydrous aluminum chloride (1.60g, 12.1 mmol) and 15 mL of freshly distilled nitrobenzene under nitrogen. The slurry was stirred at 60 °C for 10 min and formed a clear solution. To the solution were added compound **6a** (1.00 g, 2.41 mmol) and additional nitrobenzene (5 mL). The reaction turned dark green upon the completion of addition. The reaction was stirred at 60 °C for 3−4 h and allowed to cool to room temperature. The dark green solution was then poured onto a mixture of ice and 1 N HCl solution, turning purple instantaneously. The mixture was extracted with EtOAc (2 × 50 mL). The organic layers were combined, filtered, and concentrated under vacuum. The remaining nitrobenzene was subsequently removed by azeotropic distillation with H_2O (150 mL). The residue was collected and recrystallized from hot toluene (first crop) and DCM/MeOH (second crop) to give **7a**, a purple/black solid (811 mg, 1.96 mmol, 81%): mp 262−263 °C; ^{1}H NMR (300 MHz, $CDCl_3$) δ 8.87 (dd, J = 8.2, 6.9 Hz, 2H), 8.61−8.47 (m, 3H), 7.70 (d, J = 9.1 Hz, 1H), 7.68−7.59 (m, 2H), 7.58−7.55 (m, 3H), 7.53−7.41 (m, 5H), 7.33 (ddd, J = 1.0, 6.5, 9.2 Hz, 1H); IR (KBr) ν 3068, 3027, 1597, 1451, 1380, 1276, 1150 cm^{-1}; HRMS (ESI-TOF) m/z [M]$^+$ calcd for $C_{30}H_{17}Cl$ 412.1019; found 412.0990. A suitable ^{13}C NMR spectrum could not be obtained due to poor solubility.

*9,10-Diphenylindeno[1,2,3-fg]tetracene (**8a**).* To a flame-dried 100 mL round-bottom flask were added compound **7a** (100 mg, 0.242 mmol), PEPPSI-IPr (16.0 mg, 0.0235 mmol), and 10 mL of freshly distilled 1,4-dioxane. The flask was then sealed with a septum and placed under a nitrogen atmosphere. The solution was stirred at room temperature, and phenylmagnesium bromide in THF (0.24 M, 10 mL, 2.42 mmol) was added. The reaction was heated to 60 °C and stirred for 4 h. The reaction was then quenched with 1 N HCl and extracted with EtOAc (2 × 50 mL). The organic layers were combined, dried over Na_2SO_4, and concentrated under vacuum. The residue was purified by flash column chromatography (silica gel, 5% ethyl acetate in hexanes, R_f = 0.30) to give **8a** (87.5 mg, 0.192 mmol, 80%). In order to obtain the product in a solid form, the product obtained from chromatography was purified by recrystallization in DCM/MeOH to give **8a**, a purple/black solid (65.1 mg, 0.143 mmol, 60%): mp 271−272 °C; ^{1}H NMR (300 MHz, $CDCl_3$) δ 8.93 (d, J = 8.8 Hz, 2H), 8.61 (dd, J = 5.6, 3.2 Hz, 2H), 7.59 (m, 2H), 7.53 (dd, J = 5.6, 2.8 Hz, 2H), 7.36 (d, J = 9.2 Hz, 2H), 7.21 (ddd, J = 7.2, 6.4, 0.8 Hz, 2H), 7.05 (m, 6H), 6.93 (m, 4H); ^{13}C NMR (75 MHz, $CDCl_3$) δ 140.8, 140.2, 139.7, 134.0, 131.6, 131.0, 129.2, 128.9, 128.2, 127.4, 127.2, 126.7, 126.3, 124.4, 124.2, 123.8 (not all carbon signal were resolved); IR (thin film) ν 3055, 1946, 1598, 1552, 1449, 1441, 1396, 1361 cm^{-1}; HRMS (ESI-TOF) m/z [M + H]$^+$ calcd for $C_{36}H_{23}$ 455.1800; found 455.1806.

*6-Chloro-5,12-di-p-tolyl-5,12-dihydrotetracene-5,12-diol (**5b**).* 6-Chloro-5,12-di-*p*-tolyl-5,12-dihydrotetracene-5,12-diol was synthesized analogously to 6-chloro-5,12-diphenyl-5,12-dihydrotetracene-5,12-diol, compound **5a**. The crude product was carried to the next step without purification.

*5-Chloro-6,11-di-p-tolyltetracene (**6b**).* 5-Chloro-6,11-di-*p*-tolyltetracene was synthesized analogously to 5-chloro-6,11-diphenyltetracene, compound **6a**, to give an red/orange solid (2.00 g, 4.51 mmol, 88%): mp 197−198 °C; ^{1}H NMR (300 MHz, $CDCl_3$) δ 8.39 (d, J = 9.1 Hz, 1H), 8.35 (s, 1H), 7.76 (d, J = 8.1 Hz, 1H), 7.70−7.59 (m, 2H), 7.49−7.37 (m, 5H), 7.35 (s, 4H), 7.30 (d, J = 6.5 Hz, 1H), 7.27−7.24 (dd, J = 5.6, 1.9 Hz, 2H), 2.59 (s, 3H), 2.56 (s, 3H); ^{13}C NMR (75 MHz, $CDCl_3$) δ 139.1, 138.1, 137.4, 136.6, 136.2, 136.0, 132.0, 131.3, 130.5, 130.2, 130.1, 129.3, 128.8, 128.6, 128.4, 127.5, 126.9, 126.9, 126.6, 125.7, 125.3, 125.0, 125.0, 21.5, 21.5 (not all carbon signals are resolved); IR (KBr) ν 3043, 3016, 2864, 2857, 1510, 1459, 1387, 1357 cm^{-1}; HRMS (ESI-TOF) m/z [M]$^+$ calcd for $C_{32}H_{23}Cl$ 442.1488; found 442.1488.

*10-Chloro-2-methyl-9-(p-tolyl)indeno[1,2,3-fg]tetracene (**7b**).* 10-Chloro-2-methyl-9-(*p*-tolyl)indeno[1,2,3-*fg*]tetracene was synthesized analogously to 9-chloro-10-phenylindeno[1,2,3-*fg*]tetracene, compound **7a**, to give an purple solid (680 mg, 1.54 mmol, 86%): mp 197−198 °C; ^{1}H NMR (300 MHz, $CDCl_3$) δ 8.39 (d, J = 9.1 Hz, 1H), 8.35 (s, 1H), 7.76 (d, J = 8.4 Hz, 1H), 7.71−7.58 (m, 2H), 7.50−7.37 (m, 5H), 7.35 (s, 3H), 7.30 (d, J = 6.5 Hz, 1H), 7.23 (d, J = 3.0 Hz, 1H), 2.59 (s, 3H), 2.56 (s, 3H); ^{13}C NMR (75 MHz, $CDCl_3$) δ 139.1, 138.1, 137.4, 136.6, 136.2, 136.0, 132.0, 131.3, 130.5, 130.2, 130.1, 129.3, 128.8, 128.6, 128.4, 127.5, 126.9, 126.9, 126.6, 125.7, 125.3, 125.0, 125.0, 21.5, 21.5 (not all carbon signals are resolved); IR (KBr) ν 3023, 2915, 1686, 1601, 1557, 1511, 1458, 1431, 1392, 1377, 1304 cm^{-1}; HRMS (ESI-TOF) m/z [M]$^+$ calcd for $C_{32}H_{32}Cl$ 440.1332; found 440.1325.

*2-Methyl-10-phenyl-9-(p-tolyl)indeno[1,2,3-fg]tetracene (**8b**).* To a flame-dried 100 mL round-bottom flask were added **7b** (400 mg, 0.907 mmol), PEPPSI-IPr (31.0 mg, 0.0456 mmol), and 10 mL of freshly distilled 1,4-dioxane. The flask was then sealed with a septum and placed under a nitrogen atmosphere. The solution was stirred at room temperature, and phenylmagnesium bromide in THF (0.910 M, 10 mL, 9.10 mmol) was added. The reaction was heated to 60 °C and stirred for 4 h. The reaction was then quenched with 1 N HCl and extracted with EtOAc (2 × 50 mL). The organic layers were combined, dried over Na_2SO_4, and concentrated under vacuum. The residue was purified by flash column chromatography (silica gel, 5% ethyl acetate in hexanes, R_f = 0.40) to give **8b** (387 mg, 0.802 mmol, 88%). In order to obtain the product in a solid form, the product obtained from chromatography was purified by recrystallization from hot toluene/*i*PrOH (1:10) to give a purple/black solid, compound **8b** (175 mg, 0.363 mmol, 40%): mp 179−180 °C; ^{1}H NMR (300 MHz, $CDCl_3$) δ 8.89 (dd, J = 8.9, 15.9 Hz, 2H), 8.45 (d, J = 7.9 Hz, 1H), 8.40 (s, 1H), 7.62−7.53 (m, 2H), 7.45 (d, J = 9.1 Hz, 1H), 7.34 (dd, J = 11.9, 6.7 Hz, 2H), 7.20 (dd, J = 9.2, 6.4 Hz, 2H), 7.14 (dd, J = 8.3, 6.4 Hz, 1H), 7.03 (t, J = 7.4 Hz, 2H), 6.90 (dd, J = 5.2, 3.1 Hz, 2H), 6.84−6.76 (m, 4H), 2.64 (s, 3H), 2.32 (s, 3H); ^{13}C NMR (75 MHz, $CDCl_3$) δ 140.7, 140.4, 140.1, 137.2, 137.1, 136.4, 135.5, 134.0, 133.9, 131.6, 131.5, 131.1, 129.3, 129.3, 128.8, 128.5, 128.4, 127.8, 127.4, 127.2, 127.2, 127.0, 125.5, 125.2, 124.6, 124.3, 123.9, 123.8, 22.1, 21.2. (not all carbon signals are resolved); IR (KBr) ν 3042, 3021, 2912, 2857, 1599, 1558, 1511, 1456, 1434, 1396, 1360, 1294, 1133, 1021 cm^{-1}; HRMS (ESI-TOF) m/z [M]$^+$ calcd for $C_{38}H_{26}$ 482.2035; found 482.2026.

*6-Chloro-5,12-bis(4-fluorophenyl)-5,12-dihydrotetracene-5,12-diol (**5c**).* To a flame-dried 100 mL three-neck round-bottom flask was added anhydrous THF (50 mL), which was cooled to −77 °C. 1-

DOI: 10.1021/acs.joc.7b02756
J. Org. Chem. 2018, 83, 1828−1841

Bromo-4-fluorobenzene (1.965 mL, 3.130 g, 17.89 mmol) was added to THF at −77 °C followed by *n*-butyllithium (2.5 M in hexane, 6.439 mL, 24.53 mmol). The mixture was stirred at −77 °C for 10 min to form 4-fluorophenyllithium. In a flame-dried 250 mL three-neck round-bottom flask, anhydrous THF (150 mL) and 6-chloro-5,12-naphthacenequinone **4** were combined and cooled to −77 °C. The 4-fluorophenyllithium was transferred into the 250 mL round-bottom flask containing the slurry of THF and 6-chloro-5,12-naphthacenequinone via cannula at a constant flow. The mixture was allowed to react at −77 °C for 2 h and then allowed to warm to room temperature and stirred for an additional hour. The reaction was quenched with water (2 mL). The crude reaction mixture was concentrated to a solid and carried forward without purification.

*5-Chloro-6,11-bis(4-fluorophenyl)tetracene (**6c**).* The crude reaction mixture of compound **5c** was dissolved in 100 mL of dioxane and poured into a 250 mL round-bottom flask. Tin(II) chloride (5.652 g, 29.81 mmol) and $BF_3{\cdot}OEt_2$ (2.207 mL, 2.538 g, 17.89 mmol) were added to the 250 mL round-bottom flask. The reaction mixture was heated to reflux (106 °C), and reflux was maintained for 45 min. The reaction mixture was then allowed to cool to room temperature and quenched with saturated aqueous $NaHCO_3$ solution, followed by addition of solid $NaHCO_3$ until the aqueous portion was basic, as indicated by pH paper. The precipitate that formed was removed via filtration over Celite. The filtered solid was washed with chloroform (3 × 250 mL). The filtrate and chloroform washes were combined and washed once with water, once with saturated brine, dried over $MgSO_4$, concentrated, and placed under high vacuum overnight. The crude product was dissolved in boiling chloroform followed by the addition of room temperature methanol and placed in the refrigerator (5 °C) overnight. This gave compound **6c**, an orange/red solid (two steps 1.425 g, 3.160 mmol, 53%): mp 207−208 °C; ^{1}H NMR (500 MHz $CDCl_3$) δ 8.40 (d, J = 9.1 Hz, 1H), 8.28 (s, 1H), 7.77 (d, J = 8.6 Hz, 1H), 7.66−7.60 (m, 1H), 7.60−7.55 (m, 1H), 7.50−7.47 (m, 3H), 7.45−7.34 (m, 6H), 7.30−7.27 (m, 2H), 7.25−7.23 (m, 1H); ^{13}C NMR (126 MHz $CDCl_3$) δ 163.5 (d, J = 21.8 Hz), 161.5 (d, J = 20.7 Hz), 137.8 (d, J = 3.6 Hz), 137. 2, 135.1, 135.0 (d, J = 3.6 Hz), 133.0 (d, J = 7.9 Hz), 132.9 (d, J = 7.8 Hz), 132.0, 130.8, 130.3, 130.2, 129.4, 128.8, 128.6, 127.3 (d, J = 6.8 Hz), 126.6, 126.3, 125.7, 125.6, 125.5, 125.4, 125.0, 115.8 (d, J = 21.3 Hz), 114.8 (d, J = 21.3 Hz) (not all carbon signals are resolved); ^{19}F NMR (379 MHz) δ −115.43 to −115.60 (m), −116.84 (ddd, J = 14.3, 8.8, 5.6 Hz); IR (thin film) ν 3073, 1602, 1509, 1461, 1389 cm^{-1}; HRMS (GC-QTOF) m/z [M]$^+$ calcd for $C_{30}H_{17}ClF_2$ 450.0987, found 450.0972.

*10-Chloro-2-fluoro-9-(4-fluorophenyl)indeno[1,2,3-fg]tetracene (**7c**).* Compound **6c** (1.425 g, 3.165 mmol) was dissolved in chloroform (20 mL), and the solution was purged with nitrogen for 3 min. Methanesulfonic acid was then added (80 mL), and the solution was purged with nitrogen for 5 min. 2,3-Dichloro-5,6-dicyano-1,4-benzoquinone (0.862 g, 3.798 mmol) was added to the mixture of chloroform and methanesulfonic acid, and the solution was again purged with nitrogen for an additional 5 min. The reaction was stirred under nitrogen atmosphere for 3 h and wrapped in aluminum foil to shield the mixture from light. The reaction progress was monitored using ^{1}H NMR and TLC, looking for the disappearance of fluorescence of the **6c** spot. The reaction was quenched by adding saturated $NaHCO_3$ solution (approximately 100 mL; CAUTION: gas evolution, exothermic) to the reaction followed by pouring the reaction mixture into a separatory funnel containing solid $NaHCO_3$ (at least 10 g; CAUTION: gas evolution, exothermic). After being allowed to cool to room temperature, the mixture was extracted with chloroform (3 × 200 mL), and the remaining solid $NaHCO_3$ was dissolved in water. The chloroform washes were combined and washed repeatedly with saturated $NaHCO_3$ solution until the aqueous portion was clear and nearly colorless (faint yellow, usually five washes). Then the organic portion was washed repeatedly with water until the aqueous layer was no longer yellow. The organic layer was then washed with brine, dried over magnesium sulfate, concentrated, and placed under high vacuum overnight. The crude product **7c** was dissolved in boiling chloroform followed by the addition of room temperature methanol, and the mixture was placed in the refrigerator (5 °C) overnight. Compound **7c** was collected by vacuum filtration as a purple solid (1.150 g, 2.561, 81%): mp 295−296 °C; ^{1}H NMR (400 MHz $CDCl_3$) δ 8.81 (d, J = 8.9 Hz, 1H), 8.60 (d, J = 9.2 Hz, 1H), 8.46 (dd, J = 8.6, 5.3 Hz, 1H), 8.18 (dd, J = 9.9, 2.3 Hz, 1H), 7.77−7.64 (m, 2H), 7.66−7.61 (m, 1H), 7.59−7.52 (m, 1H), 7.44−7.33 (m, 3H), 7.30−7.27 (m, 2H), 7.25−7.15 (m, 1H);); ^{19}F NMR (379 MHz, $CDCl_3$) δ −115.68 (td, J = 9.3, 5.2 Hz), −115.94 to −116.09 (m); IR (thin film) ν 2917, 1602, 1507, 1460, 1395 cm^{-1}; HRMS (GC-QTOF) m/z [M]$^+$ calcd for $C_{30}H_{15}ClF_2$ 448.0830; found 448.0813. A suitable ^{13}C NMR spectrum could not be obtained due to poor solubility.

*2-Fluoro-9-(4-fluorophenyl)-10-phenylindeno[1,2,3-fg]tetracene (**8c**).* In a flame-dried 250 mL two-neck round-bottom flask, anhydrous THF (150 mL), compound **7c** (1.0981 g, 2.451 mmol), and PEPPSI-IPr (0.067 g, 0.09 mmol) were added, and the solution was purged with nitrogen for 10 min. The reaction was heated to 65 °C, at which point phenylmagnesium bromide was added (1 M in THF, 3.677 mL, 0.667 g, 3.677 mmol). The solution was maintained at 65 °C under a nitrogen atmosphere and wrapped in aluminum foil overnight. The reaction was monitored by ^{1}H NMR. Upon complete consumption of **7c**, the reaction was allowed to cool to room temperature and quenched with water (2 mL). THF was removed in vacuo, and the resulting solid was dissolved in chloroform (600 mL). The organic extract was washed once with saturated $NaHCO_3$ solution, once with water, once with brine, dried over $MgSO_4$, concentrated, and placed under high vacuum overnight. Crude compound **8c** was dissolved in boiling chloroform followed by the addition of room temperature methanol and placed in the refrigerator (5 °C) overnight. Compound **8c** was collected by vacuum filtration as a purple solid (1.076 g, 2.193 mmol, 90%): phase change 265 °C, sublimes 278 °C; ^{1}H NMR (500 MHz $CDCl_3$) δ 8.87 (d, J = 8.9 Hz, 1H), 8.82 (d, J = 8.9 Hz, 1H), 8.54 (dd, J = 8.5, 5.3 Hz, 1H), 8.29 (dd, J = 9.9, 2.4 Hz, 1H), 7.71−7.58 (m, 2H), 7.48−7.34 (m, 2H), 7.28−7.20 (m, 4H), 7.17−7.08 (m, 2H), 6.97−6.93 (m, 2H), 6.93−6.84 (m, 2H), 6.85−6.67 (m, 1H); ^{13}C NMR (125 MHz $CDCl_3$) δ 133.2, 133.1, 131.6, 129.4, 129.2, 129.0, 128.0, 127.7, 127.4, 126.5, 124.9, 124.8, 124.7 (d, J = 6.8 Hz), 123.3, 114.23 (d, J = 21.4 Hz), 113.1 (d, J = 22.8 Hz), 111.8 (d, J = 24.9 Hz) (not all carbon signals are resolved); ^{19}F NMR (379 MHz, $CDCl_3$) δ −116.27 (td, J = 9.3, 5.2 Hz), −117.61 to −117.81 (m); IR (thin film) ν 2957, 2916, 2849, 1601, 1508, 1469, 1460 cm^{-1}; HRMS (GC-QTOF) m/z [M]+ calcd for $C_{36}H_{20}F_2$ 490.1533; found 490.1526.

*6-Chloro-5,12-bis(4-(trifluoromethyl)phenyl)-5,12-dihydrotetracene-5,12-diol (**5d**).* 6-Chloro-5,12-bis(4-(trifluoromethyl)phenyl)-5,12-dihydrotetracene-5,12-diol was synthesized analogously to 6-chloro-5,12-bis(4-fluorophenyl)-5,12-dihydrotetracene-5,12-diol, compound **5c**. The product was carried to the next step without purification.

*5-Chloro-6,11-bis(4-(trifluoromethyl)phenyl)tetracene (**6d**).* 5-Chloro-6,11-bis(4-(trifluoromethyl)phenyl)tetracene (**6d**) was synthesized analogously to 5-chloro-6,11-bis(4-fluorophenyl)tetracene, compound **6c**, to give an orange/red solid (two steps, 2.309 g, 4.191 mmol, 46%): mp 249−250 °C; ^{1}H NMR (500 MHz $CDCl_3$) δ 8.38 (dd, J = 8.3, 1 Hz, 1H), 8.21 (s, 1H), 7.96 (d, J = 7.9 Hz, 1H), 7.82 (d, J = 7.9 Hz, 1H), 7.79 (d, J = 8.7 Hz, 1H), 7.66 (d, J = 7.8 Hz, 2H), 7.61 (d, J = 7.8 Hz, 2H), 7.57−7.45 (m, 3H), 7.38 (dd, J = 8.7, 6.1 Hz, 1H), 7.30 (dd, J = 7.1, 3.2 Hz, 2H); ^{13}C NMR (125 MHz $CDCl_3$) δ 146.0, 143.1, 136.9, 134.9, 131.8, 131.7, 131.5, 130.9, 130.4, 130.3 (q, 36 Hz), 129.6, 129.5 (q, 36 Hz), 129.0, 128.7, 128.6, 127.6, 127.0, 126.3, 126.1, 126.1, 125.2, 124.9, 125.7 (q, 4 Hz), 124.7 (q, 4 Hz), 124.5 (q, 270 Hz), 124.3 (q, 270 Hz) (not all carbon signals are resolved); ^{19}F NMR (379 MHz, $CDCl_3$) δ −63.36, −63.62; IR (thin film) ν 3074, 1616, 1461, 1406, 1324 cm^{-1}; HRMS (GC-QTOF) m/z [M]$^+$ calcd for $C_{32}H_{17}ClF_6$ 550.0923; found 550.0941.

*10-Chloro-2-(trifluoromethyl)-9-(4-(trifluoromethyl)phenyl)-indeno[1,2,3-fg]tetracene (**7d**).* 10-Chloro-2-(trifluoromethyl)-9-(4-(trifluoromethyl)phenyl)indeno[1,2,3-*fg*]tetracene was synthesized analogously to 10-chloro-2-fluoro-9-(4-fluorophenyl)indeno[1,2,3-*fg*]-tetracene, compound **7c**, to give a purple/black solid (0.8479 g, 1.545 mmol, 40%): mp 259−260 °C; ^{1}H NMR (400 MHz $CDCl_3$) δ 8.89 (d, J = 8.9 Hz, 1H), 8.84 (d, J = 8.8 Hz, 1H), 8.71 (s, 1H), 8.64 (d, J = 8.2 Hz, 1H), 8.58 (d, J = 9.1 Hz, 1H), 7.87−7.81 (m, 2H), 7.82−7.68

DOI: 10.1021/acs.joc.7b02756
J. Org. Chem. 2018, 83, 1828−1841

(m, 3H), 7.64−7.55 (m, 4H), 7.41 (dd, J = 10.1, 6.4 Hz, 1H); ^{19}F NMR (379 MHz, $CDCl_3$) δ −63.05, −63.45; IR (thin film) ν 3071, 1679, 1617, 1595, 1432, 1405, 1324 cm^{-1}; HRMS (GC-QTOF) m/z [M]$^+$ calcd for $C_{32}H_{15}ClF_6$ 548.0766; found 548.0774. A suitable ^{13}C NMR spectrum could not be obtained due to poor solubility.

*10-Phenyl-2-(trifluoromethyl)-9-(4-(trifluoromethyl)phenyl)-indeno[1,2,3-fg]tetracene (**8d**).* In a flame-dried 250 mL three-neck round-bottom flask, anhydrous toluene (150 mL), compound **7d** (0.8038 g, 1.467 mmol), and PEPPSI-IPr (0.040 g, 0.05868 mmol) were added, and the solution was purged with nitrogen for 10 min. The reaction was heated to 65 °C, at which point phenylmagnesium bromide was added (1 M in THF, 2.200 mL, 2.200 mmol). The solution was maintained at 65 °C under a nitrogen atmosphere wrapped in aluminum foil overnight. The reaction was monitored by ^{1}H NMR. Upon complete consumption of **7d**, the reaction was allowed to cool to room temperature and quenched with water (2 mL). Toluene was removed in vacuo, and the resulting solid was dissolved in chloroform (600 mL). The chloroform solution was washed once with saturated $NaHCO_3$ solution, once with water, once with brine, dried over $MgSO_4$, concentrated, and placed under high vacuum overnight. The crude product was dissolved in boiling chloroform followed by the addition of room temperature methanol and placed in the refrigerator (5 °C) overnight. Compound **8d** was collected by vacuum filtration, a purple/black solid (0.7947 g, 1.346 mmol, 92%): mp 228−229 °C; ^{1}H NMR (400 MHz $CDCl_3$) δ 8.94 (d, J = 9.0 Hz, 1H), 8.90 (d, J = 8.9 Hz, 1H), 8.82 (s, 1H), 8.71 (d, J = 8.2 Hz, 1H), 7.82 (d, J = 8.1 Hz, 1H), 7.73−7.64 (m, 2H), 7.41 (d, J = 9.0 Hz, 1H), 7.37−7.25 (m, 5H), 7.22−7.14 (m, 1H), 7.14−6.96 (m, 4H), 6.92 (dd, J = 8.1, 1.3 Hz, 1H); ^{13}C NMR (125 MHz $CDCl_3$) δ 143.9, 142.2, 141.6, 140.3, 134.2, 133.6, 131.8, 131.6, 130.2, 129.6, 129.5, 129.5, 129.4, 128.9, 128.8, 128.7, 128.5, 128.4, 128.4, 127.5, 127.0, 125.2, 125.4, 124.2 (q, J = 3.7 Hz), 124.0, 123.7, 123.5, 120.6, 120.6 (not all carbon signals are resolved); ^{19}F NMR (379 MHz, $CDCl_3$) δ −62.92, −64.91; IR (thin film) ν 3060, 235l, 1615, 1551, 1448, 1364, 1324 cm^{-1}; HRMS (GC-QTOF) m/z [M]$^+$ calcd for $C_{38}H_{20}F_6$ 590.1469; found 590.1450. Due to poor solubility, not all expected ^{13}C NMR signals were observed.

*6-Chloro-5,12-bis(4-methoxyphenyl)-5,12-dihydrotetracene-5,12-diol (**5e**).* 6-Chloro-5,12-bis(4-methoxyphenyl)-5,12-dihydrotetracene-5,12-diol was synthesized analogously to 6-chloro-5,12-bis(4-fluorophenyl)-5,12-dihydrotetracene-5,12-diol, compound **5c**. The product was carried to the next step without purification.

*5-Chloro-6,11-bis(4-methoxyphenyl)tetracene (**6e**).* 5-Chloro-6,11-bis(4-methoxyphenyl)tetracene (**6e**) was synthesized analogously to 5-chloro-6,11-bis(4-fluorophenyl)tetracene, compound **6c**, to give an orange/red solid (two steps, 1.0323 g, 2.173 mmol, 55%): mp 205−206 °C; ^{1}H NMR (500 MHz $CDCl_3$) δ 8.40 (dd, J = 8.3, 1 Hz, 1H), 8.36 (s, 1H), 7.77 (d, J = 8.7 Hz, 1H), 7.74−7.67 (m, 1H), 7.68−7.62 (m, 1H), 7.49−7.40 (m, 3H), 7.39−7.30 (m, 3H), 7.29−7.23 (m, 2H), 7.23−7.14 (m, 2H), 7.15−7.06 (m, 2H), 4.01 (s, 2H), 3.98 (s, 3H); ^{13}C NMR (125 MHz $CDCl_3$) δ 159.2, 158.8, 137.8, 135.6, 134.2, 132.5, 132.4, 132.2, 131.3, 130.5, 130.4, 130.1, 129.5, 128.8, 128.6, 127.4, 126.9, 126.9, 126.5, 125.8, 125.3, 125.1, 125.0, 114.0, 113.1, 55.4, 55.3. (not all carbon signals are resolved); IR (thin film) ν 2953, 2834, 1607, 1511, 1460, 1388 cm^{-1}; HRMS (GC-QTOF) m/z [M]$^+$ calcd for $C_{32}H_{23}ClO_2$ 474.1387; found 474.1382.

*10-Chloro-2-methoxy-9-(4-methoxyphenyl)indeno[1,2,3-fg]-tetracene (**7e**).* 10-Chloro-2-methoxy-9-(4-methoxyphenyl)indeno-[1,2,3-*fg*]tetracene was synthesized analogously to 10-chloro-2-fluoro-9-(4-fluorophenyl)indeno[1,2,3-*fg*]tetracene, compound **7c**, to give an purple/black solid (0.341 g, 0.721 mmol, 69%): mp 260−264 °C; ^{1}H NMR (400 MHz $CDCl_3$) δ 8.83 (d, J = 5.1 Hz, 1H), 8.81 (d, J = 5.2 Hz, 1H), 8.63 (d, J = 9.1 Hz, 1H), 8.43 (d, J = 8.5 Hz, 1H), 8.08 (d, J = 2.3 Hz, 1H), 7.77 (d, J = 9.1 Hz, 1H), 7.67 (dd, J = 9.3, 5.9 Hz, 1H), 7.60 (dd, J = 9.3, 5.9 Hz, 1H), 7.55 (dd, J = 8.7, 6.9 Hz, 1H), 7.41−7.30 (m, 3H), 7.18−7.09 (m, 2H), 7.05 (dd, J = 8.5, 2.3 Hz, 1H), 4.07 (s, 3H), 4.01 (s, 3H); IR (thin film) ν 3058, 2934, 2832, 1606,1576, 1510, 1460, 1431, 1397 cm^{-1}; HRMS (GC-QTOF) m/z [M]$^+$ calcd for $C_{32}H_{21}ClO_2$ 472.1230, found 472.1237. Due to poor solubility, a ^{13}C NMR spectrum could not be obtained.

*2-Methoxy-9-(4-methoxyphenyl)-10-phenylindeno[1,2,3-fg]-tetracene (**8e**).* 2-Methoxy-9-(4-methoxyphenyl)-10-phenylindeno-[1,2,3-*fg*]tetracene, compound **8e**, was synthesized analogously to 2-fluoro-9-(4-fluorophenyl)-10-phenylindeno[1,2,3-*fg*]tetracene, compound **8c**, to give a purple solid (0.2020 g, 0.393 mmol, 54%): mp 212−213 °C; ^{1}H NMR (400 MHz $CDCl_3$) δ 8.85 (d, J = 8.9 Hz, 1H), 8.83 (d, J = 8.9 Hz, 1H), 8.47 (d, J = 8.5 Hz, 1H), 8.15 (d, J = 2.3 Hz, 1H), 7.58 (ddd, J = 8.8, 6.4, 1.0 Hz, 2H), 7.55 (ddd, J = 8.8, 6.4, 1.0 Hz, 2H), 7.44 (d, J = 9.1 Hz, 1H), 7.36 (d, J = 9.1 Hz, 1H), 7.23−7.17 (m, 2H), 7.14−7.04 (m, 4H), 6.93 (dd, J = 8.0, 1.2 Hz, 2H), 6.57 (dd, J = 8.6, 2 Hz, 1H), 4.07 (s, 3H), 3.84 (s, 3H); ^{13}C NMR (125 MHz $CDCl_3$) δ 159.1, 157.8, 141.5, 141.2, 140.6, 139.2, 134.4, 133.9, 133.0, 132.7, 132.5, 131.6, 131.1, 130.8, 129.3, 129.3, 128.8, 128.1, 127.4, 127.2, 127.1, 126.0, 124.7, 124.7, 124.4, 124.3, 123.8, 123.5, 113.0, 111.7, 110.9, 55.8, 55.3. (not all carbon signals are resolved); IR (thin film) ν 3000, 2954, 2834, 1675, 1607, 1573, 1511, 1461, 1441, 1411, 1389, 1360, 1315 cm^{-1}; HRMS (GC-QTOF) m/z [M]$^+$ calcd for $C_{38}H_{26}O_2$ 514.1933; found 514.1926.

*6-Chloro-5,12-bis(4-ethylphenyl)-5,12-dihydrotetracene-5,12-diol (**5f**).* 6-Chloro-5,12-bis(4-ethylphenyl)-5,12-dihydrotetracene-5,12-diol was synthesized analogously to 6-chloro-5,12-diphenyl-5,12-dihydrotetracene-5,12-diol, compound **5a**. The crude product was carried to the next step without purification.

*5-Chloro-6,11-bis(4-ethylphenyl)tetracene (**6f**).* 5-Chloro-6,11-bis-(4-ethylphenyl)tetracene was synthesized analogously to 5-chloro-6,11-diphenyltetracene, compound **6a**, to give an red/orange solid (0.343 g, 0.730 mmol, 73% yield over two steps): mp 160−161 °C; ^{1}H NMR ($CDCl_3$, 500 MHz) δ 8.39 (d, J = 9.1 Hz, 1H), 8.36 (s, 1H), 7.77 (d, J = 8.5 Hz, 1H), 7.68 (dt, J = 7.3, 2.5 Hz, 1H), 7.63 (dt, J = 6.0, 2.4 Hz, 1H), 7.51−7.47 (m, 2H), 7.46−7.39 (m, 3H), 7.32 (dd, J = 8.3, 6.6 Hz, 1H), 7.28−7.22 (m, 2H), 2.96−2.82 (m, 4H), 1.48−1.38 (m, 6H); ^{1}H NMR (400 MHz, CD_2Cl_2) δ 8.37−8.35(m, 2H), 7.76 (d, J = 8.4 Hz, 1H), 7.65−7.62 (m, 1H), 7.61−7.59 (m, 1H), 7.51−7.49 (m, 2H), 7.46−7.44 (m, 1H), 7.42−7.40 (m, 2H), 7.39−7.35 (m, 4H), 7.33−7.31 (m, 1H), 7.24 (dt, J = 6.8, 2.9, Hz, 2H), 2.86 (dq, J = 15.1, 7.6 Hz, 4H), 1.41 (dt, J = 10.9, 7.6 Hz, 6H); ^{13}C NMR ($CDCl_3$, 125 MHz) δ 143.6, 143.0, 139.2, 138.2, 136.4, 136.1, 132.0, 131.4, 130.5, 130.1, 129.4, 128.6, 128.0, 127.1, 126.9, 126.6, 125.7, 125.3, 125.0, 125.0, 125.0, 28.8, 15.7, 15.6 (not all carbon signals are resolved); IR (KBr) ν 3022, 2964, 2930, 1511, 1460, 1389, 1360, 1316 cm^{-1}; HRMS (ESI-TOF) m/z [M]$^+$ calcd for $C_{34}H_{27}Cl$ 470.1801; found 470.1835.

*10-Chloro-2-ethyl-9-(4-ethylphenyl)indeno[1,2,3-fg]tetracene (**7f**).* 10-Chloro-2-ethyl-9-(4-ethylphenyl)indeno[1,2,3-*fg*]tetracene was synthesized analogously to 10-chloro-2-fluoro-9-(4-fluorophenyl)-indeno[1,2,3-*fg*]tetracene, compound **7a**, to give an purple/black solid (405 mg, 0.86 mmol, 67%): mp 246−250 °C; ^{1}H NMR (400 MHz, $CDCl_3$) δ 8.85 (d, J = 8.8 Hz, 1H), 8.85 (d, J = 8.8 Hz, 1H), 8.57 (d, J = 9.1 Hz, 1H), 8.40 (d, J = 7.9 Hz, 1H), 8.30 (s, 1H), 7.73 (d, J = 9.1 Hz, 1H), 7.64 (dd, J = 8.8, 6.5 Hz, 1H), 7.58 (dd, J = 8.8, 6.5 Hz, 1H), 7.51 (dd, J = 9.1, 6.4 Hz, 1H), 7.41−7.37 (m, 2H), 7.35−7.28 (m, 4H), 2.97−2.79 (m, 4H), 1.49−1.37 (m, 6H); ^{13}C NMR (100 MHz, $CDCl_3$) δ 143.4, 143.3, 139.7, 138.5, 138.1, 137.3, 134.3, 131.8, 131.7, 131.7, 131.3, 131.0, 130.8, 129.4, 129.3, 129.1, 128.6, 127.7, 127.5, 127.4, 127.0, 126.6, 126.0, 124.9, 124.3, 124.1, 123.9, 123.0, 29.5, 28.8, 16.0, 15.7(not all carbon signals are resolved); IR (Thin film) ν 3045, 2963, 2930, 2871, 1677, 1615, 1559, 1511, 1459, 1435, 1394, 1375, 1337, 1305 cm^{-1}; HRMS (GC-QTOF) m/z [M]$^+$ calcd for $C_{34}H_{25}Cl$ 468.1645; found 468.1664.

*2-Ethyl-9-(4-ethylphenyl)-10-phenylindeno[1,2,3-fg]tetracene (**8f**).* Compound **8f** was synthesized analogously to 2-fluoro-9-(4-fluorophenyl)-10-phenylindeno[1,2,3-*fg*]tetracene, compound **8c**, to give an purple/black solid to give an purple solid (31 mg, 0.061 mmol, 74%): mp 165−167 °C; ^{1}H NMR (400 MHz, $CDCl_3$) δ 8.94 (dd, 2H, J = 20.8, 8.8 Hz), 8.52 (d, 1H, J = 8.0 Hz), 8.42 (s, 1H), 7.61−7.54 (m, 2H), 7.43−7.34 (m, 3H), 7.22−7.18 (m, 2H), 7.11−7.01 (m, 3H), 6.94−6.91 (m, 2H), 6.86−6.82 (m, 4H), 2.94 (q, J = 7.6 Hz, 2H), 2.62 (t, J = 7.6 Hz, 2H),1.47 (t, J = 7.6 Hz, 3H), 1.31 (t, J = 7.6 Hz, 3H); IR (thin film) ν 3054, 2961, 2927, 2869, 1602, 1553, 1511, 1458, 1440, 1397, 1362, 755, 737, 700 cm^{-1}; HRMS (GC-QTOF) m/z [M]$^+$ calcd

DOI: 10.1021/acs.joc.7b02756
J. Org. Chem. 2018, 83, 1828−1841

for $C_{40}H_{30}$ 510.2348, found 510.2366. Due to poor solubility, a ^{13}C NMR spectrum could not be obtained.

*6-Chloro-5,12-bis(4-propylphenyl)-5,12-dihydrotetracene-5,12-diol (**5g**).* 6-Chloro-5,12-bis(4-propylphenyl)-5,12-dihydrotetracene-5,12-diol was synthesized analogously to 6-chloro-5,12-diphenyl-5,12-dihydrotetracene-5,12-diol, compound **5a**. The crude product was carried to the next step without purification.

*5-Chloro-6,11-bis(4-propylphenyl)tetracene (**6g**).* 5-Chloro-6,11-bis(4-propylphenyl)tetracene was synthesized analogously to 5-chloro-6,11-diphenyltetracene, compound **6a**, to give an red/orange solid (0.800 g, 1.50 mmol, 80% yield over two steps): mp 167−168 °C; ^1H NMR ($CDCl_3$, 500 MHz) δ 8.39 (dd, J = 8.2 Hz, 1 Hz, 1H), 8.35 (s, 1H), 7.76 (d, J = 8.7 Hz, 1H), 7.72−7.65 (m, 1H), 7.65−7.59 (m, 1H), 7.50−7.44 (m, 3H), 7.43−7.39 (m, 2H), 7.39−7.34 (m, 3H), 7.34−7.28 (m, 2H), 7.26−7.23 (m, 2H), 2.91−2.70 (m, 4H), 1.93−1.76 (m, 4H), 1.15−1.04 (m, 6H); ^{13}C NMR ($CDCl_3$, 125 MHz) δ 142.1, 141.3, 139.2, 138.1, 136.4, 136.0, 131.9, 131.2, 131.2, 130.5, 130.2, 130.0, 129.3, 128.8, 128.6, 127.7, 127.4, 126.8, 126.5, 125.6, 125.3, 125.0, 125.0, 124.9, 37.9, 37.9, 24.6, 24.5, 14.0, 13.8 (not all carbon signals are resolved); IR (KBr) ν 3074, 3023, 2929, 2958, 2870, 1511, 1461, 1407, 1389, 1361, 1316 cm^{-1}; HRMS (GC-QTOF) m/z $[M]^+$ calcd for $C_{36}H_{31}Cl$ 498.2114; found 498.2131.

*10-Chloro-2-propyl-9-(4-propylphenyl)indeno[1,2,3-fg]tetracene (**7g**).* 10-Chloro-2-propyl-9-(4-propylphenyl)indeno[1,2,3-*fg*]tetracene (**7g**) was synthesized analogously to 9-chloro-10-phenylindeno[1,2,3-*fg*]tetracene, compound **7a**, to give a purple/black solid (14 mg, 0.032 mmol, 47%): mp 200−202 °C; ^1H NMR (400 MHz, $CDCl_3$) δ 8.86 (d, J = 9.0 Hz, 1H), 8.83 (d, J = 9.1 Hz, 1H), 8.58 (d, J = 9.1 Hz, 1H), 8.40 (d, J = 7.9 Hz, 1H), 8.29 (s, 1H), 7.74 (d, J = 9.1 Hz, 1H), 7.64 (dd, J = 6.5 Hz, 2.1 Hz, 1H); 7.59 (dd, J = 6.5 Hz, 2.1 Hz, 1H), 7.51 (dd, J = 9.1, 6.5 Hz, 1H), 7.40−7.29 (m, 6H), 2.89−2.76 (m, 4H), 1.96−1.72 (m, 4H), 1.23−0.90 (m, 6H); IR (KBr) ν 3044, 2958, 2929, 2870, 1682, 1615, 1600, 1558, 1511, 1462, 1434, 1393, 1378, 1338, 1304 cm^{-1}; HRMS (GC-QTOF) m/z $[M]^+$ calcd for $C_{36}H_{29}Cl$ 496.1958; found 496.1964. Due to poor solubility, a ^{13}C NMR spectrum could not be obtained.

*10-Phenyl-2-propyl-9-(4-propylphenyl)indeno[1,2,3-fg]tetracene (**8g**).* Compound **8g** was synthesized analogously to 2-fluoro-9-(4-fluorophenyl)-10-phenylindeno[1,2,3-*fg*]tetracene, compound **8c**, to give a purple/black solid (32 mg, 0.059 mmol, 74%): mp 193−195 °C; ^1H NMR (400 MHz, $CDCl_3$) δ 8.90 (dd, 2H, J = 19.6, 10.8 Hz), 8.48 (d, 1H, J = 8.0 Hz), 8.40 (s, 1H), 7.61−7.54 (m, 2H), 7.39−7.33 (m, 3H), 7.22−7.17 (m, 2H), 7.11−7.01 (m, 3H), 6.94−6.92 (m, 2H), 6.83 (s, 4H), 2.88 (t, J = 7.6 Hz, 2H), 2.54 (t, J = 7.6 Hz, 2H), 1.88 (sext, J = 7.2 Hz, 2H), 1.71 (sext, J = 7.2 Hz, 2H), 1.09 (m, 6H); ^{13}C NMR (100 MHz, $CDCl_3$) δ 141.5, 140.8, 140.5, 140.2, 140.1, 137.6, 137.4, 134.2, 131.7, 131.6, 129.4, 129.3, 128.9, 128.6, 127.3, 127.2, 127.1, 127.0, 126.1, 124.7, 124.3, 123.9, 123.9, 38.7, 38.1, 25.0, 24.6, 14.3, 14.0 (not all carbon signals are resolved); IR (thin film) ν 3055, 2957, 2928, 2869, 1600, 1557, 1511, 1498, 1440, 1397, 1377, 1362, 1339, 1298, 1264, 1138, 1021, 970, 794, 755, 738, 700 cm^{-1}; HRMS (GC-QTOF) m/z $[M]^+$ calcd for $C_{42}H_{34}$ 538.2661; found 538.2683.

*9-(4-Fluorophenyl)-10-phenylindeno[1,2,3-fg]tetracene (**8h**).* To a flame-dried 100 mL round-bottom flask were **7a** (300 mg, 0.727 mmol), PEPPSI-IPr (25.0 mg, 0.0368 mmol), and 10 mL of freshly distilled 1,4-dioxane. The flask was then sealed with a septum and placed under a nitrogen atmosphere. The solution was stirred at room temperature, and *p*-fluorophenylmagnesium bromide in THF (0.72 M, 10 mL, 7.27 mmol) was added. The reaction was heated to 60 °C and stirred for 4 h. The reaction was then quenched with 1 N HCl and extracted with EtOAc (2 × 50 mL). The organic layers were combined, dried over Na_2SO_4, and concentrated under vacuum. The residue was purified by flash column chromatography (silica gel, 2% ethyl acetate in hexanes (R_f = 0.30) to give impure compound **8h** (222 mg, 0.470 mmol, 65%). In order to obtain pure product in a solid form, the product obtained from chromatography was purified by recrystallization in DCM/MeOH to give compound **8h**, a purple/black solid (176 mg, 0.372 mmol, 51%): mp 243−244 °C; ^1H NMR (300 MHz, $CDCl_3$) δ 8.92 (d, J = 8.9 Hz, 2H), 8.60 (dd, J = 5.6, 3.2 Hz, 2H), 7.65−7.57 (m, 2H), 7.53 (dd, J = 5.6, 3.1 Hz, 2H), 7.36 (d, J = 9.1 Hz, 2H), 7.24−7.15 (m, 3H), 7.10 (t, J = 7.3 Hz, 2H), 6.96−6.79 (m, 4H), 6.72 (t, J = 8.8 Hz, 2H); ^{13}C NMR (75 MHz, $CDCl_3$) δ 161.35 (d, J = 221 Hz), 140.5, 140.3, 139.7, 139.6, 139.4, 134.1, 133.2, 133.1, 131.6, 129.2, 128.9, 128.8, 127.5, 127.5, 127.3, 126.9, 126.8, 126.3, 124.6, 124.6, 124.3, 123.9, 123.8, 114.1 (d, J = 21.5 Hz) (not all carbon signals are resolved, including the expected 3 bond C−F coupling); ^{19}F NMR (379 MHz, $CDCl_3$) δ −117.88 (tt, J = 9.3, 5.8 Hz); IR (KBr) ν 3035, 3033, 1597, 1556, 1503, 1396, 1212, 1133 cm^{-1}; HRMS (ESI-TOF) m/z $[M]^+$ calcd for $C_{36}H_{21}F$ 472.1627; found 472.1614.

*9-Phenyl-10-(p-tolyl)indeno[1,2,3-fg]tetracene (**8i**).* To a flame-dried 100 mL round-bottom flask were added **7b** (791 mg, 1.92 mmol), PEPPSI-IPr (65.0 mg, 0.0957 mmol), and 15 mL of freshly distilled 1,4-dioxane. The flask was then sealed with a septum and placed under a nitrogen atmosphere. The solution was stirred at room temperature, and *p*-methylphenylmagnesium bromide in THF (1.28 M, 15 mL, 19.2 mmol) was added. The reaction was heated to 60 °C and stirred for 4 h. The reaction was then quenched with 1 N HCl and extracted with EtOAc (2 × 50 mL). The organic layers were combined, dried over Na_2SO_4, and concentrated under vacuum. The residue was passed through a silica plug, eluted with 5% ethyl acetate in hexanes, and concentrated under vacuum. The crude product was further purified by recrystallization in hot xylenes/*i*PrOH to give compound **8i**, a purple/black solid (598 mg, 1.28 mmol, 67%): mp 180−181 °C; ^1H NMR (300 MHz, $CDCl_3$) δ 8.92 (d, J = 8.8 Hz, 2H), 8.60 (dd, J = 5.7, 3.2 Hz, 2H), 7.63−7.55 (m, 2H), 7.52 (dd, J = 5.7, 3.1 Hz, 2H), 7.47 (d, J = 9.1 Hz, 1H), 7.36 (d, J = 9.1 Hz, 1H), 7.25−7.17 (m, 2H), 7.15−7.10 (m, 1H), 7.02 (t, J = 7.5 Hz, 2H), 6.92−6.87 (m, 2H), 6.84−6.75 (m, 4H), 2.32 (s, 3H); ^{13}C NMR (75 MHz, $CDCl_3$) δ 141.1, 140.9, 140.4, 139.7, 139.6, 137.0, 135.6, 134.0, 134.0, 131.6, 131.4, 130.9, 130.8, 129.4, 129.3, 129.0, 128.9, 128.3, 127.9, 127.5, 127.4, 127.0, 126.7, 126.6, 125.5, 124.6, 124.3, 124.3, 124.2, 123.8, 21.2. (not all carbon signals are resolved); IR (KBr) ν 3041, 3022, 2892, 2852, 1558, 1511, 1469, 1451, 1440, 1430, 1396, 1360, 1297, 1136, 1020, 968 cm^{-1}; HRMS (ESI-TOF) m/z $[M]^+$ calcd for $C_{37}H_{24}$ 468.1878; found 468.1907.

*9-(Naphthalen-1-yl)-10-phenylindeno[1,2,3-fg]tetracene (**8j**).* To a flame-dried 100 mL round-bottom flask were added **7a** (800 mg, 1.94 mmol), PEPPSI-IPr (65.0 mg, 0.0957 mmol), and 15 mL of freshly distilled 1,4-dioxane. The flask was then sealed with a septum and placed under a nitrogen atmosphere. The solution was stirred at room temperature, and α-naphthylmagnesium bromide in THF (1.29 M, 15 mL, 19.4 mmol) was added. The reaction was heated to 60 °C and stirred for 4 h. The reaction was then quenched with 1 N HCl and extracted with EtOAc (2 × 50 mL). The organic layers were combined, dried over Na_2SO_4, and concentrated under vacuum. The residue was passed through a silica plug, eluted with 5% ethyl acetate in hexanes, and concentrated under vacuum. The crude was further purified by recrystallization in hot chloroform/MeOH to give compound **8j**, a purple/black solid (438 mg, 0.868 mmol, 45%): mp 243−244 °C; ^1H NMR (300 MHz, $CDCl_3$) δ 8.95 (t, J = 9.2 Hz, 2H), 8.64 (dt, J = 6.0, 3.1 Hz, 2H), 7.71 (d, J = 8.1 Hz, 1H), 7.64−7.53 (m, 5H), 7.35 (dd, J = 10.9, 4.0 Hz, 1H), 7.29−7.20 (m, 3H), 7.19−7.06 (m, 4H), 6.99 (d, J = 8.4 Hz, 1H), 6.91 (d, J = 6.3 Hz, 2H), 6.79−6.71 (m, 1H), 6.32 (d, J = 6.6 Hz, 2H); ^{13}C NMR (75 MHz, $CDCl_3$) δ 141.0, 139.7, 138.8, 138.7, 137.9, 134.2, 134.1, 134.0, 133.1, 131.4, 131.2, 131.1, 130., 129.8, 129.3, 129.0, 128.4, 127.7, 127.7, 127.6, 127.5, 127.3, 126.9, 126.8, 126.2, 125.9, 125.6, 125.4, 125.3, 125.0, 124.9, 124.7, 124.4, 124.3, 124.3, 123.9, 123.7 (not all carbon signal were resolved); IR (KBr) ν 3041, 1595, 1596, 1558, 1504, 1469, 1452, 1439, 1382, 1360, 1298, 1256, 1187, 1171, 1139, 1016, 965 cm^{-1}; HRMS (ESI-TOF) m/z $[M]^+$ calcd for $C_{40}H_{24}$ 504.1878; found 504.1840.

*N,N-Dimethyl-4-(10-phenylindeno[1,2,3-fg]tetracen-9-yl)aniline (**8k**).* To a flame-dried 100 mL round-bottom flask were added **7a** (500 mg, 1.21 mmol), PEPPSI-IPr (41.0 mg, 0.0603 mmol), and 10 mL of freshly distilled 1,4-dioxane. The flask was then sealed with a septum and placed under a nitrogen atmosphere. The solution was stirred at room temperature, and *p*-*N*,*N*-dimethylaminophenylmagnesium bromide in THF (1.21 M, 10 mL, 12.1 mmol) was added. The reaction

DOI: 10.1021/acs.joc.7b02756
J. Org. Chem. 2018, 83, 1828−1841

was heated to 60 °C and stirred for 4 h. The reaction was then quenched with 1 N HCl and extracted with EtOAc (2 × 50 mL). The combined organic layer was then washed with saturated $NaHCO_3$ solution and brine, dried over Na_2SO_4, and concentrated under vacuum. The crude was further purified by recrystallization in DCM/MeOH to give **8k**, a purple/black solid (286 mg, 0.575 mmol, 47%): mp 238−241 °C; ^{1}H NMR (300 MHz, $CDCl_3$) δ 8.92 (dd, J = 8.6, 3.3 Hz, 2H), 8.60 (dd, J = 5.6, 3.3 Hz, 2H), 7.63−7.59 (m, 3H), 7.52 (dd, J = 5.7, 3.1 Hz, 2H), 7.37 (d, J = 9.1 Hz, 1H), 7.25−7.16 (m, 2H), 7.12−7.02 (m, 3H), 6.96−6.90 (m, 2H), 6.79−6.72 (m, 2H), 6.42 (d, J = 8.7 Hz, 2H), 2.97 (s, 3H); ^{13}C NMR (75 MHz, $CDCl_3$) δ 149.1, 142.0, 141.2, 140.7, 139.8, 139.6, 134.5, 133.9, 132.1, 131.5, 130.9, 130.4, 129.7, 129.4, 129.1, 128.9, 128.4, 127.5, 127.3, 127.1, 126.6, 126.5, 126.0, 124.9, 124.2, 124.1, 123.8, 123.7, 112.2, 40.9 (not all carbon signals are resolved); IR (KBr) ν 3857, 3747, 3654, 3043, 2786, 1610, 1517, 1468, 1443, 1394, 1344, 1298, 1191, 1166 cm^{-1}; HRMS (ESI-TOF) m/z [M]$^+$ calcd for $C_{38}H_{27}N$ 497.2143; found 497.2135.

*9-(4-Methoxyphenyl)-10-phenylindeno[1,2,3-fg]tetracene (**8l**).* To a flame-dried 100 mL round-bottom flask were added **7a** (400 mg, 0.969 mmol), dehydrated *para*-methoxyphenylboronic acid (468 mg, 1.16 mmol), PEPPSI-IPr (13.0 mg, 0.0191 mmol), potassium carbonate (670 mg, 4.85 mmol), and 50 mL of freshly distilled toluene under nitrogen. The solution was then heated to 90 °C and stirred for 24 h. The mixture was then passed through a Celite plug to remove insoluble solids and was rinsed with ethyl acetate. The organic extracts were concentrated under vacuum. The residue was passed through a silica plug and eluted with 10% ethyl acetate in hexanes to remove a small amount of unconsumed starting material. The crude product was further purified by recrystallization in DCM/MeOH to give **8l**, a purple/black solid (414 mg combined from two crops of crystals, 0.854 mmol, 88%): mp 158−159 °C; ^{1}H NMR (300 MHz, $CDCl_3$) δ 8.92 (d, J = 8.9 Hz, 2H), 8.61 (dd, J = 5.7, 3.2 Hz, 2H), 7.59 (ddd, J = 8.9, 2.3, 1.2 Hz, 2H), 7.53 (dd, J = 5.7, 3.1 Hz, 2H), 7.47 (d, J = 9.2 Hz, 1H), 7.36 (d, J = 9.2 Hz, 1H), 7.24−7.18 (m, 2H), 7.15−7.05 (m, 3H), 6.96−6.91 (m, 2H), 6.83 (d, J = 8.7 Hz, 2H), 6.57 (d, J = 8.7 Hz, 2H), 3.84 (s, 3H); ^{13}C NMR (75 MHz, $CDCl_3$) δ 157.8, 140.9, 140.8, 140.5, 139.7, 139.7, 134.3, 134.0, 132.6, 132.4, 131.6, 131.0, 130.8, 129.4, 129.3, 129.0, 128.9, 128.3, 127.5, 127.4, 127.2, 126.7, 126.0, 124.7, 124.4, 124.2, 123.8, 112.9, 55.3 (not all carbon signals are resolved); IR (KBr) ν 3435, 3039, 2958, 2839, 1607, 1501, 1276, 1233, 1183, 1041, 1012 cm^{-1}; HRMS (ESI-TOF) m/z [M]$^+$ calcd for $C_{37}H_{24}O$ 484.1827; found 484.1811.

*N,N-Dimethyl-4-(3-methyl-10-(p-tolyl)indeno[1,2,3-fg]tetracen-9-yl)aniline (**8m**).* To a flame-dried 100 mL round-bottom flask were added **7b** (400 mg, 0.998 mmol), PEPPSI-IPr (34.0 mg, 0.0500 mmol), and 10 mL of freshly distilled 1,4-dioxane. The flask was then sealed with a septum and placed under a nitrogen atmosphere. The solution was stirred at room temperature, and *p*-*N*,*N*-dimethylaminophenylmagnesium bromide in THF (1.00 M, 10 mL, 10.0 mmol) was added. The reaction was heated to 60 °C and stirred for 4 h. The reaction was then quenched with 1 N HCl and extracted with EtOAc (2 × 50 mL). The combined organic layer was then washed with saturated $NaHCO_3$ solution and brine, dried over Na_2SO_4, and concentrated under vacuum. The crude was further purified by recrystallization in hot toluene/*i*PrOH (1:10) to give **8m**, a purple/black solid (353 mg, 0.672 mmol, 67%): mp 259−263 °C; ^{1}H NMR (300 MHz, $CDCl_3$) δ 8.92 (dd, J = 8.6, 3.3 Hz, 2H), 8.46 (d, J = 7.8 Hz, 1H), 8.40 (s, 1H), 7.58 (d, J = 9.4 Hz, 3H), 7.44 (d, J = 9.2 Hz, 1H), 7.32 (d, J = 7.8 Hz, 1H), 7.20 (dd, J = 15.6, 7.5 Hz, 2H), 6.86−6.77 (m, 4H), 6.76−6.68 (m, 2H), 6.40 (d, J = 8.5 Hz, 2H), 2.97 (s, 6H), 2.65 (s, 3H), 2.31 (s, 3H); IR (KBr) 3025, 2916, 2857, 2794, 1610, 1557, 1514, 1456, 1396, 1348, 1192, 1161 cm^{-1}; HRMS (ESI-TOF) m/z [M]$^+$ calcd for $C_{40}H_{31}N$ 525.2457; found 525.2431. Due to poor solubility, a ^{13}C NMR spectrum could not be obtained.

*10-(4-Fluorophenyl)-2-methyl-9-(p-tolyl)indeno[1,2,3-fg]-tetracene (**8n**).* To a flame-dried 100 mL round-bottom flask were added **7b** (400 mg, 0.907 mmol), PEPPSI-IPr (31.0 mg, 0.0456 mmol), and 10 mL of freshly distilled 1,4-dioxane. The flask was then sealed with a septum and placed under a nitrogen atmosphere. The solution was stirred at room temperature, and *p*-fluorophenylmagnesium bromide in THF (0.907 M, 10 mL, 9.07 mmol) was added. The reaction was heated to 60 °C and stirred for 4 h. The reaction was then quenched with 1 N HCl and extracted with EtOAc (2 × 50 mL). The organic layers were combined, dried over Na_2SO_4, and concentrated under vacuum. The residue was purified by flash column chromatography (silica gel, 5% ethyl acetate in hexanes, R_f 0.35) to give **8n** (278 mg, 0.555 mmol, 60%). In order to obtain the product in a solid form, the product obtained from chromatography was purified by recrystallization in hot toluene/*i*PrOH (1:10) to give compound **8n**, a purple/black solid (114 mg, 0.227 mmol, 25%): mp 231−232 °C; ^{1}H NMR (300 MHz, $CDCl_3$) δ 8.89 (dd, J = 17.7, 8.9 Hz, 2H), 8.45 (d, J = 7.9 Hz, 1H), 8.40 (s, 1H), 7.58 (td, J = 15.8, 8.0 Hz, 2H), 7.44 (d, J = 9.0 Hz, 1H), 7.35 (t, J = 8.3 Hz, 2H), 7.20 (dd, J = 9.1, 6.3 Hz, 2H), 6.92−6.69 (m, 8H), 2.64 (s, 3H), 2.38 (s, 3H); ^{13}C NMR (75 MHz, $CDCl_3$) δ 140.0, 139.3, 137.3, 136.5, 135.9, 134.1, 134.0, 133.1, 133.0, 131.5, 129.3, 129.0, 128.7, 128.5, 128.0, 127.6, 127.3, 125.3, 124.8, 124.4, 123.93, 123.87, 114.1, 113.8 (d, J = 21.5 Hz), 22.1, 21.6 (not all carbon signals are resolved, the carbon *ipso* to the fluorine could not be extracted from noise); ^{19}F NMR (379 MHz, $CDCl_3$) δ 118.23 (tt, J = 9.1, 5.6 Hz); IR (KBr) ν 3022, 2918, 2857, 1599, 1556, 1508, 1456, 1432, 1396, 1355, 1295, 1215, 1152, 1018 cm^{-1}; HRMS (ESI-TOF) m/z [M]$^+$ calcd for $C_{38}H_{25}F$ 500.1940, found 500.1949.

■ ASSOCIATED CONTENT

Supporting Information

The Supporting Information is available free of charge on the ACS Publications website at DOI: 10.1021/acs.joc.7b02756.

Computational results, copies of NMR spectra for new compounds, X-ray diffraction data (PDF)

X-ray data for **8b**, **8c**, **8d**, **8e**, and **8h** CIF)

■ AUTHOR INFORMATION

Corresponding Authors

*E-mail: cramer@umn.edu.

*E-mail: cdouglas@umn.edu.

ORCID

Lafe J. Purvis: 0000-0001-6538-2343

Soumen Ghosh: 0000-0003-0850-4855

Christopher J. Cramer: 0000-0001-5048-1859

Christopher J. Douglas: 0000-0002-1904-6135

Present Address

†Chemical & Analytical Development, Suzhou Novartis Pharma Technology Co., Ltd., #18 Tonglian Road, Riverside Industrial Park, Changshu Economic Development Zone, Changshu/Jiangsu Province, 215537, China.

Notes

The authors declare no competing financial interest.

■ ACKNOWLEDGMENTS

This work was supported in part by the U.S. Department of Energy, Office of Science, Office of Basic Energy Sciences, Division of Chemical Sciences, Geosciences, and Biosciences, the Office of Science, Office of Workforce Development for Teachers and Scientists, Office of Science Graduate Student Research (SCGSR) program, and the Office of Advanced Scientific Computing Research through the Scientific Discovery through Advanced Computing (SciDAC) program under Award Number DE-SC0008666. The SCGSR program is administered by the Oak Ridge Institute for Science and Education for the DOE under contract number DE-SC0014664. The National Science Foundation is acknowledged for support via the MRSEC program (DMR-1006566) and for

DOI: 10.1021/acs.joc.7b02756
J. Org. Chem. 2018, 83, 1828−1841

a grant to purchase the Bruker-AXS D8 Venture single-crystal diffractometer (MRI-1229400), along with the University of Minnesota. The authors acknowledge the Minnesota Supercomputing Institute (MSI) at the University of Minnesota for providing resources that contributed to the research results reported within this paper, and Professor Laura Gagliardi (UMN) for helpful discussions. C.J.D. thanks DuPont for a Young Professor Award.

REFERENCES

(1) Zhou, Y.; Ding, L.; Shi, K.; Dai, Y. Z.; Ai, N.; Wang, J.; Pei, J. *Adv. Mater.* **2012**, *24*, 957.
(2) Zhang, J.; Li, C. Z.; Williams, S. T.; Liu, S.; Zhao, T.; Jen, A. K. *J. Am. Chem. Soc.* **2015**, *137*, 2167.
(3) Kim, Y.; Park, G.; Choi, S.; Lee, D.; Cho, M.; Choi, D. *J. Mater. Chem. C* **2017**, *5*, 7182.
(4) Hwang, Y. J.; Li, H.; Courtright, B. A.; Subramaniyan, S.; Jenekhe, S. A. *Adv. Mater.* **2016**, *28*, 124.
(5) Meng, D.; Sun, D.; Zhong, C.; Liu, T.; Fan, B.; Huo, L.; Li, Y.; Jiang, W.; Choi, H.; Kim, T.; Kim, J. Y.; Sun, Y.; Wang, Z.; Heeger, A. J. *J. Am. Chem. Soc.* **2016**, *138*, 375.
(6) Hendsbee, A. D.; Sun, J. P.; Rutledge, L. R.; Hill, I. G.; Welch, G. C. *J. Mater. Chem. A* **2014**, *2*, 4198.
(7) Jones, B. A.; Ahrens, M. J.; Yoon, M. H.; Facchetti, A.; Marks, T. J.; Wasielewski, M. R. *Angew. Chem., Int. Ed.* **2004**, *43*, 6363.
(8) Chase, D. T.; Fix, A. G.; Rose, B. D.; Weber, C. D.; Nobusue, S.; Stockwell, C. E.; Zakharov, L. N.; Lonergan, M. C.; Haley, M. M. *Angew. Chem., Int. Ed.* **2011**, *50*, 11103.
(9) Buchholtz, F.; Zelichenok, A.; Krongauz, V. *Macromolecules* **1993**, *26*, 906.
(10) Li, M. M.; Liu, Y. T.; Ni, W.; Liu, F.; Feng, H. R.; Zhang, Y. M.; Liu, T. T.; Zhang, H. T.; Wan, X. J.; Kan, B.; Zhang, Q.; Russell, T. P.; Chen, Y. S. *J. Mater. Chem. A* **2016**, *4*, 10409.
(11) Rananaware, A.; Gupta, A.; Kadam, G.; Duc La, D.; Bilic, A.; Xiang, W.; Evans, R. A.; Bhosale, S. V. *Mater. Chem. Front.* **2017**, *1*, 2511.
(12) Gupta, A.; Rananaware, A.; Srinivasa Rao, P.; Duc La, D.; Bilic, A.; Xiang, W.; Li, J.; Evans, R. A.; Bhosale, S. V.; Bhosale, S. V. *Mater. Chem. Front.* **2017**, *1*, 1600.
(13) Liu, F.; Zhou, Z.; Zhang, C.; Vergote, T.; Fan, H.; Liu, F.; Zhu, X. *J. Am. Chem. Soc.* **2016**, *138*, 15523.
(14) Eftaiha, A. F.; Sun, J. P.; Hill, I. G.; Welch, G. C. *J. Mater. Chem. A* **2014**, *2*, 1201.
(15) Kondratenko, M.; Moiseev, A. G.; Perepichka, D. F. *J. Mater. Chem.* **2011**, *21*, 1470.
(16) Li, S. X.; Yan, J. L.; Li, C. Z.; Liu, F.; Shi, M. M.; Chen, H. Z.; Russell, T. P. *J. Mater. Chem. A* **2016**, *4*, 3777.
(17) Shen, Z.; Xu, B.; Liu, P.; Hu, Y.; Yu, Y.; Ding, H.; Kloo, L.; Hua, J.; Sun, L.; Tian, H. *J. Mater. Chem. A* **2017**, *5*, 1242.
(18) Jiang, H.; Ferrara, G.; Zhang, X.; Oniwa, K.; Islam, A.; Han, L.; Sun, Y. J.; Bao, M.; Asao, N.; Yamamoto, Y.; Jin, T. *Chem. - Eur. J.* **2015**, *21*, 4065.
(19) Deng, Y.; Xu, B.; Castro, E.; Fernandez-Delgado, O.; Echegoyen, L.; Baldridge, K. K.; Siegel, J. S. *Eur. J. Org. Chem.* **2017**, *2017*, 4338.
(20) Lee, C. H.; Plunkett, K. N. *Org. Lett.* **2013**, *15*, 1202.
(21) Zhu, X. J.; Bheemireddy, S. R.; Sambasivarao, S. V.; Rose, P. W.; Torres Guzman, R.; Waltner, A. G.; DuBay, K. H.; Plunkett, K. N. *Macromolecules* **2016**, *49*, 127.
(22) Lu, R. Q.; Zheng, Y. Q.; Zhou, Y. N.; Yan, X. Y.; Lei, T.; Shi, K.; Zhou, Y.; Pei, J.; Zoppi, L.; Baldridge, K. K.; Siegel, J. S.; Cao, X. Y. *J. Mater. Chem. A* **2014**, *2*, 20515.
(23) Gu, X.; Luhman, W. A.; Yagodkin, E.; Holmes, R. J.; Douglas, C. J. *Org. Lett.* **2012**, *14*, 1390.
(24) We are currently analyzing unpublished data that demonstrate asymmetric indenotetracene's potential as an electron-transport material in organic photovoltaics.
(25) To remove inorganic tin from the product, the reaction mixture is made basic, filtered over diatomaceous earth, and further purified via recrystallization from hot chloroform with methanol.
(26) Miao, Q.; Chi, X.; Xiao, S.; Zeis, R.; Lefenfeld, M.; Siegrist, T.; Steigerwald, M. L.; Nuckolls, C. *J. Am. Chem. Soc.* **2006**, *128*, 1340.
(27) Zhai, L.; Shukla, R.; Wadumethrige, S. H.; Rathore, R. *J. Org. Chem.* **2010**, *75*, 4748.
(28) Grzybowski, M.; Skonieczny, K.; Butenschon, H.; Gryko, D. T. *Angew. Chem., Int. Ed.* **2013**, *52*, 9900.
(29) Smet, M.; Van Dijk, J.; Dehaen, W. *Synlett* **1999**, *1999*, 495.
(30) Eversloh, C. L.; Avlasevich, Y.; Li, C.; Mullen, K. *Chem. - Eur. J.* **2011**, *17*, 12756.
(31) Lakshminarayana, A. N.; Chang, J.; Luo, J.; Zheng, B.; Huang, K. W.; Chi, C. *Chem. Commun.* **2015**, *51*, 3604.
(32) Wu, J.; Pisula, W.; Mullen, K. *Chem. Rev.* **2007**, *107*, 718.
(33) Avlasevich, Y.; Kohl, C.; Mullen, K. *J. Mater. Chem.* **2006**, *16*, 1053.
(34) Zhai, L.; Shukla, R.; Rathore, R. *Org. Lett.* **2009**, *11*, 3474.
(35) Yagodkin, E.; Douglas, C. J. *Tetrahedron Lett.* **2010**, *51*, 3037.
(36) O'Brien, C. J.; Kantchev, E. A.; Valente, C.; Hadei, N.; Chass, G. A.; Lough, A.; Hopkinson, A. C.; Organ, M. G. *Chem. - Eur. J.* **2006**, *12*, 4743.
(37) Compounds **8a−i** were characterized by ^{1}H, ^{13}C, ^{19}F NMR and IR. HRMS was done via QTOF and ESI. Single-crystal X-ray structures were obtained for compounds **8a−e**,**h**.
(38) Dexter, D. L. *J. Chem. Phys.* **1953**, *21*, 836.
(39) CIFs found in the Supporting Information
(40) The degree of indenotetracene core overlap and π-stacking distance were measured from the solved crystal structures.
(41) Coropceanu, V.; Cornil, J.; da Silva Filho, D. A.; Olivier, Y.; Silbey, R.; Bredas, J. L. *Chem. Rev.* **2007**, *107*, 926.
(42) Sonar, P.; Williams, E. L.; Singh, S. P.; Manzhos, S.; Dodabalapur, A. *Phys. Chem. Chem. Phys.* **2013**, *15*, 17064.
(43) Lan, L. Y.; Chen, Z. M.; Ying, L.; Huang, F.; Cao, Y. *Org. Electron.* **2016**, *30*, 176.
(44) Valenti, G.; Bruno, C.; Rapino, S.; Fiorani, A.; Jackson, E. A.; Scott, L. T.; Paolucci, F.; Marcaccio, M. *J. Phys. Chem. C* **2010**, *114*, 19467.
(45) Zhu, X. J.; Yuan, B. X.; Plunkett, K. N. *Tetrahedron Lett.* **2015**, *56*, 7105.
(46) Bheemireddy, S. R.; Ubaldo, P. C.; Rose, P. W.; Finke, A. D.; Zhuang, J.; Wang, L.; Plunkett, K. N. *Angew. Chem., Int. Ed.* **2015**, *54*, 15762.
(47) Zhou, K.; Dong, H.; Zhang, H. L.; Hu, W. *Phys. Chem. Chem. Phys.* **2014**, *16*, 22448.
(48) Li, H. Y.; Earmme, T.; Subramaniyan, S.; Jenekhe, S. A. *Adv. Energy Mater.* **2015**, *5*, 1402041.
(49) Zhou, F.; Jehoulet, C.; Bard, A. J. *J. Am. Chem. Soc.* **1992**, *114*, 11004.
(50) Kulshreshtha, C.; Kim, W. G.; Lampande, R.; Huh, H. D.; Chae, M.; Kwon, H. J. *J. Mater. Chem. A* **2013**, *1*, 4077.
(51) Zhao, Y.; Truhlar, D. *Theor. Chem. Acc.* **2008**, *120*, 215.
(52) Kwon, O. K.; Park, J. H.; Kim, D. W.; Park, S. K.; Park, S. Y. *Adv. Mater.* **2015**, *27*, 1951.
(53) Shi, X.; Liu, S.; Liu, C.; Hu, Y.; Shi, S.; Fu, N.; Zhao, B.; Wang, Z.; Huang, W. *Chem. - Asian J.* **2016**, *11*, 2188.
(54) Lu, X.; Fan, S.; Wu, J.; Jia, X.; Wang, Z. S.; Zhou, G. *J. Org. Chem.* **2014**, *79*, 6480.
(55) Frischmann, P. D.; Mahata, K.; Wurthner, F. *Chem. Soc. Rev.* **2013**, *42*, 1847.
(56) Huss, A. S.; Pappenfus, T.; Bohnsack, J.; Burand, M.; Mann, K. R.; Blank, D. A. *J. Phys. Chem. A* **2009**, *113*, 10202.
(57) Li, C.; Liu, M.; Pschirer, N. G.; Baumgarten, M.; Mullen, K. *Chem. Rev.* **2010**, *110*, 6817.
(58) Experiments to measure singlet fission in asymmetric indenotetracenes are currently underway.
(59) Zimmerman, P. M.; Bell, F.; Casanova, D.; Head-Gordon, M. *J. Am. Chem. Soc.* **2011**, *133*, 19944.

DOI: 10.1021/acs.joc.7b02756
J. Org. Chem. 2018, 83, 1828−1841

(60) Congreve, D. N.; Lee, J.; Thompson, N. J.; Hontz, E.; Yost, S. R.; Reusswig, P. D.; Bahlke, M. E.; Reineke, S.; Van Voorhis, T.; Baldo, M. A. *Science* **2013**, *340*, 334.
(61) Ehrler, B.; Walker, B. J.; Bohm, M. L.; Wilson, M. W.; Vaynzof, Y.; Friend, R. H.; Greenham, N. C. *Nat. Commun.* **2012**, *3*, 1019.
(62) See Table S15.
(63) Ide, J.; Mereau, R.; Ducasse, L.; Castet, F.; Olivier, Y.; Martinelli, N.; Cornil, J.; Beljonne, D. *J. Phys. Chem. B* **2011**, *115*, 5593.
(64) Vura-Weis, J.; Ratner, M. A.; Wasielewski, M. R. *J. Am. Chem. Soc.* **2010**, *132*, 1738.
(65) Adamo, C.; Barone, V. *J. Chem. Phys.* **1999**, *110*, 6158.
(66) Arbeloa, F. L.; Ojeda, R. P.; Arbeloa, L. I. *J. Lumin.* **1989**, *44*, 105−112.
(67) Grabolle, M.; Spieles, M.; Lesnyak, V.; Gaponik, N.; Eychmuller, A.; Resch-Genger, U. *Anal. Chem.* **2009**, *81*, 6285.
(68) Perdew, J. P.; Burke, K.; Ernzerhof, M. *Phys. Rev. Lett.* **1996**, *77*, 3865.
(69) Frisch, M. J.; Trucks, G. W.; Schlegel, H. B.; Scuseria, G. E.; Robb, M. A.; Cheeseman, J. R.; Scalmani, G.; Barone, V.; Mennucci, B.; Petersson, G. A.; Nakatsuji, H.; Caricato, M.; Li, X.; Hratchian, H. P.; Izmaylov, A. F.; Bloino, J.; Zheng, G.; Sonnenberg, J. L.; Hada, M.; Ehara, M.; et al. *Gaussian 09*; Gaussian, Inc.: Wallingford, CT, 2009.
(70) Valiev, M.; Bylaska, E. J.; Govind, N.; Kowalski, K.; Straatsma, T. P.; Van Dam, H. J. J.; Wang, D.; Nieplocha, J.; Apra, E.; Windus, T. L.; de Jong, W. A. *Comput. Phys. Commun.* **2010**, *181*, 1477.

DOI: 10.1021/acs.joc.7b02756
J. Org. Chem. 2018, 83, 1828−1841